SUPPORTING INFORMATION

Cluster Growth Reactions: Structures and Bonding of Metal-Rich Metallaheteroboranes Containing Heavier Chalcogen Elements

Chandan Nandi,[a] Arindam Roy,[a] Ketaki Kar,[a] Marie Cordier[b] and Sundargopal Ghosh[a]*

[a]Department of Chemistry, Indian Institute of Technology Madras, Chennai 600036, India. Tel: +91 44-22574230; Fax: +91 44-22574202; E-mail: sghosh@iitm.ac.in

[b]Université *de Rennes, CNRS, Institut des Sciences Chimiques de Rennes, UMR 6226, F-35000 Rennes, France*

Table of contents

I.1 Supplementary Data

I.2 Spectroscopic Details

II Computational Details

I.1 Supplementary Data

Table S1. Selected structural parameters and ^{11}B NMR values for polyhedral and macropolyhedral metallaboranes and metallaheteroboranes.

Clusters	Structural parameters				Spectroscopic details		
	Av. $d_{B\text{-}E}$ [Å][a]		Av. $d_{B\text{-}B}$ [Å]		^{11}B NMR (ppm)		
	Expt.	Calc.	Expt.	Calc.	Expt.	Calc.	Ref.
3/3´	2.23	2.19	1.78	1.78	35.6, 30.4, 24.5, 2.6	36.4, 27.8, 25.8, 4.5	[b]
4/4´	2.42	2.43	1.77	1.79	38.9, 27.3, 26.6, 8.1	28.1, 22.1, 19.0, 4.6	[b]
5/5´	2.24	2.14	1.77	1.76	24.7, 23.5	27.4, 23.4	[b]
6/6´	2.44	2.43	1.82	1.75	27.2[c]	29.5, 29.1	[b]
8/8´	2.44	2.47	1.78	1.76	50.0, 39.4, 35.8, 14.9, 5.6	63.4, 40.7, 34.7, 26.1, 18.4, 12.1, 11.3	[b]
10/10´	1.85	1.88	1.81	1.80	34.8, 30.7, 26.2, 6.9	43.1, 33.0, 19.2, 6.3	[b]
I	-	-	1.81	-	56.3, 37.8, 29.0, 25.4, 16.1, 14.2, 10.6, 3.8, -10.6, -12.0	-[d]	1
II	1.87	1.90	1.92	-	23.6, 19.3, 17.8, 6.1, 2.3, -3.2, -4.2, -6.5, -7.6, -10.2, -12.6, -14.4, -15.6, -16.8, -18.0, -35.7	-[d]	2
III	-	-	1.81	-	63.0, 26.9, 22.3, 15.7, 5.4, 0.6, -0.6, -6.9, -9.9, -10.3, -12.9, -17.0, -21.3, -28.2	-[d]	3
IV	2.24	-	1.81	-	39.4, 3.9	-[d]	4
V	2.51	-	1.81	-	-	-[d]	5
VI	2.35	-	1.80	-	-3.6, -8.5	-[d]	6

Av. = average, *d* = distance, [a] E = S, Se or Te, [b] this work, [c] accidental overlap of ^{11}B chemical shifts, [-d] no data available.

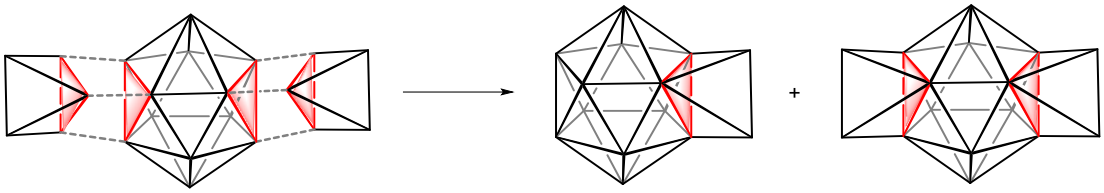

Figure S1. Schematic representation of cluster fusion for **3**-**6**

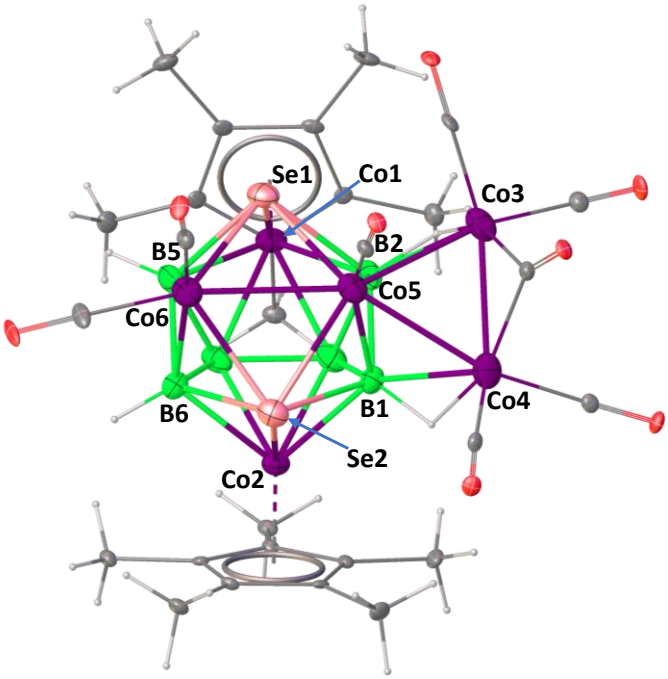

Figure S2. Molecular structure and labeling diagram of **3**. Thermal ellipsoids of the core are set at the 40% probability level. Selected bond lengths [Å] and angles (deg): B5-B6 1.784(12), B1-B2 1.773(12), B1-Co2 2.128(8), B1-Co5 2.135(9), B1-Co4 2.229(8), B6-Co6 2.216(9), B1-Se2 2.249(8), B2-Se1 2.282(8), B5-Se1 2.160(8); B2-B1-Co2 117.4(5), B2-B1-Co5 65.7(4), Co2-B1-Co5 122.4(4), B2-B1-Se2 115.0(5), Co2-B1-Se2 63.9(2), Co3-Co5-Co4 58.63(4), B2-Co5-B1 49.0(3).

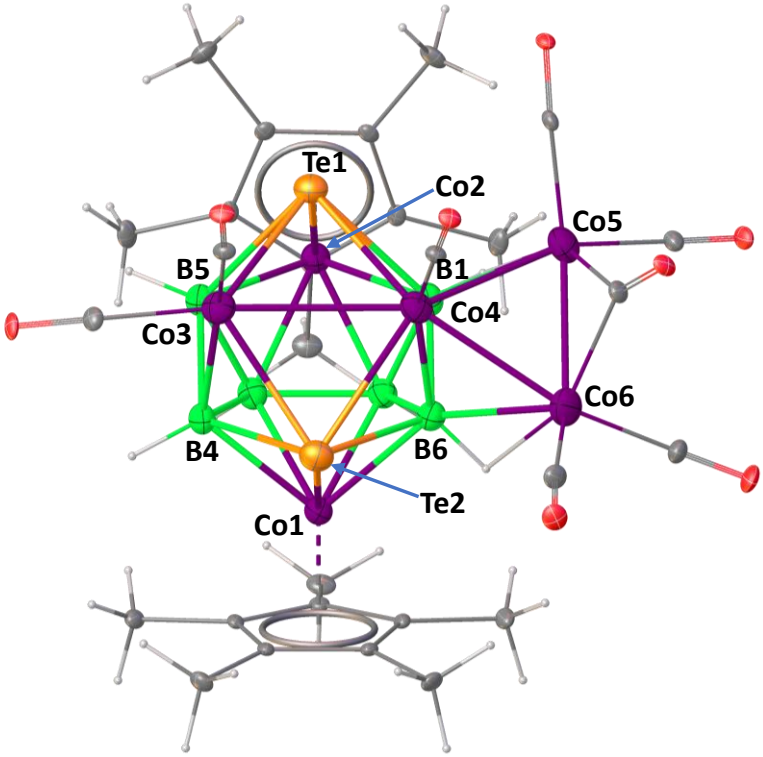

Figure S3. Molecular structure and labeling diagram of **4**. Thermal ellipsoids of the core are set at the 40% probability level. Selected bond lengths [Å] and angles (deg): B1-B6 1.741(5), B4-B5 1.773(5), B1-Co2 2.139(4), B1-Co4 2.126(4), B1-Te1 2.439(4), B4-Te2 2.414(4), B4-Co1 2.150(4), Co5-Co6 2.4319(7), Co4-Te1 2.5058(5), Co3-Co4 2.7470(7); B6-B1- Co4 66.03(18), B6-B1-Co2 118.9(2), B6-B1-Te1 117.5(2), Co4-B1-Te1 66.16(11), Co5-B1-Te1 100.67(15), B5-B4-Co1 117.8(2), Te2-Co3-Te1 107.553(19).

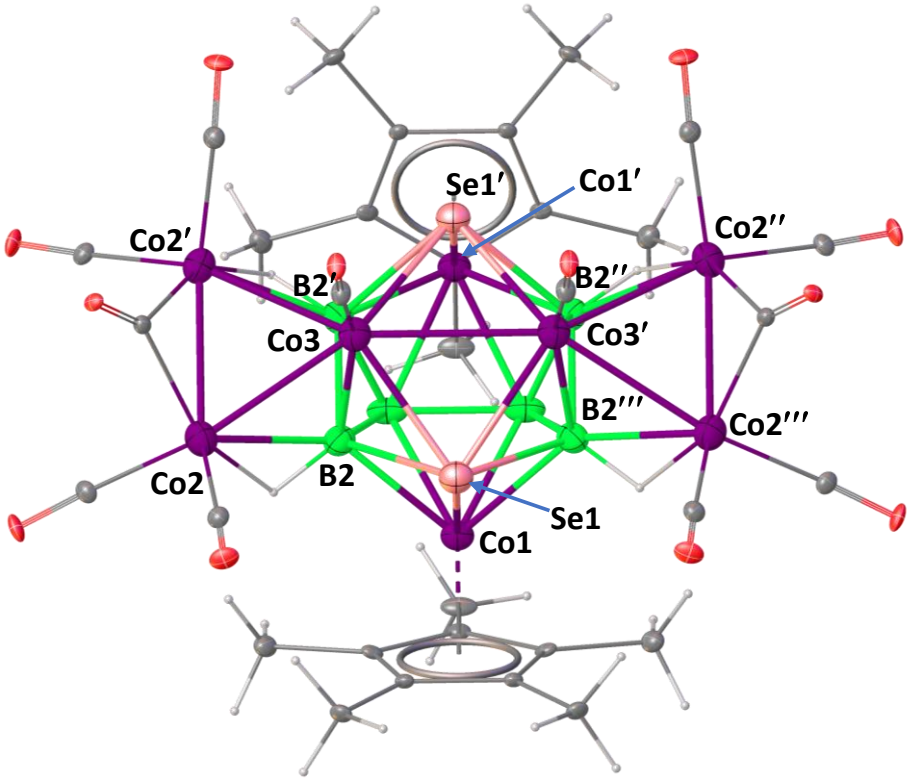

Figure S4. Molecular structure and labeling diagram of **5**. Thermal ellipsoids of the core are set at the 40% probability level. Selected bond lengths [Å] and angles (deg): Co1-B2 2.118(9), Co1-Se1 2.3177(18), Co2-Co3 2.4896(17), Co3-B2 2.117(10), Co3-Co3′ 2.651(3), Se1-B2 2.242(9), B2-B2′ 1.73(2); B2′-Co1′-B2″ 94.2(5), B2-Co1-Se1 60.5(3), B2-Co2-Co2′ 81.0(3), B2-Co2-Co3 52.9(2), Co2-Co3-Co2′ 58.33(6).

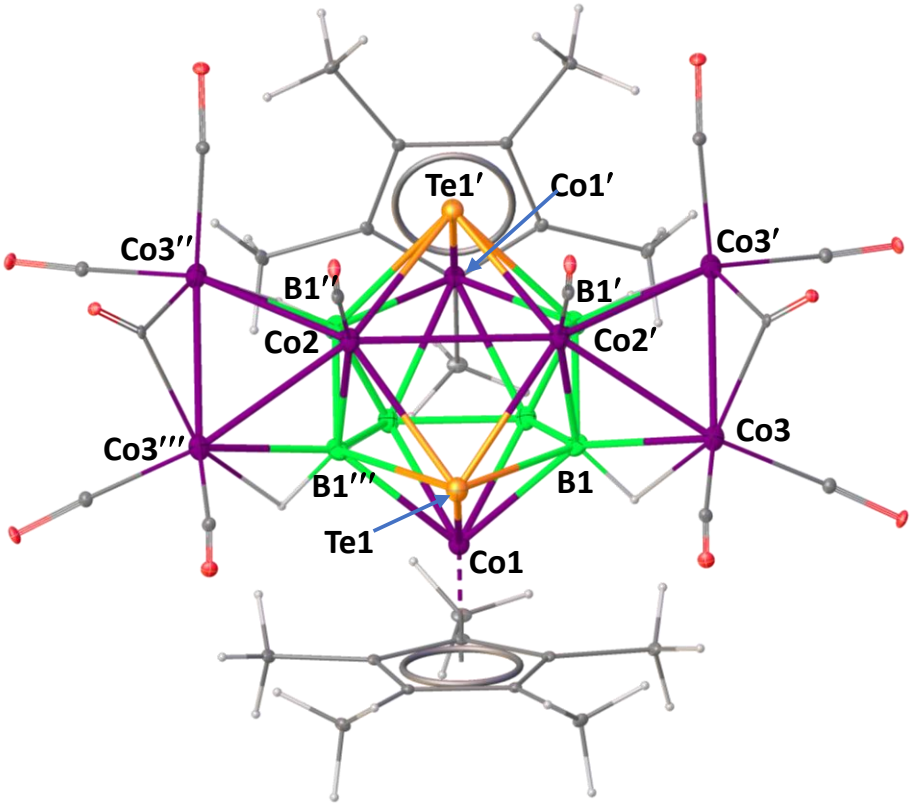

Figure S5. Molecular structure and labeling diagram of **6**. Thermal ellipsoids of the core are set at the 40% probability level. Selected bond lengths [Å] and angles (deg): Te1-B1 2.444(5), Te1-Co2 2.4646(6), Te1-Co1 2.4661(9), Co1-B1 2.141(5), Co2-B1‴ 2.137(5), Co2-Co3″ 2.4901(9), Co2-Co2′ 2.7938(15); B1-Te1-B1‴ 81.7(2), B1-Te1-Co2′ 51.61(11), Co2-Te1-Co2′ 69.05(3), B1-Te1-Co1 51.69(11), Co2-Te1-Co1 99.28(3), B1-Co1-Te1 63.63(12).

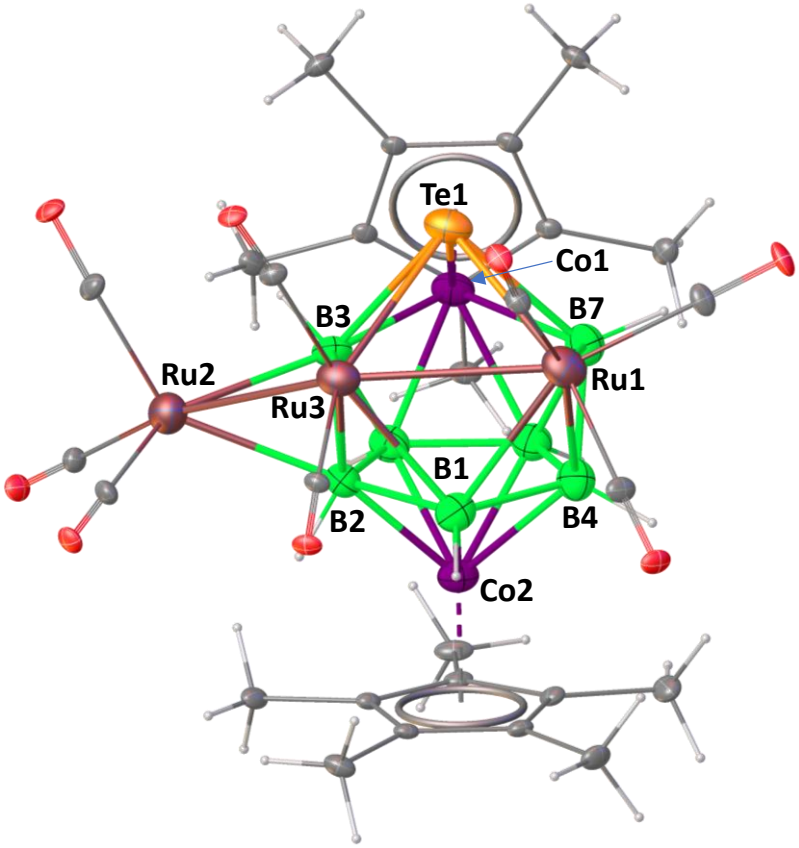

Figure S6. Molecular structure and labeling diagram of **8**. Thermal ellipsoids of the core are set at the 40% probability level. One CH_2Cl_2 molecule is omitted for clarity. Selected bond lengths (Å) and angles (°): Co1-B3 2.103(7), Co1-B7 2.197(7), Co1-Te1 2.4692(9), Co2-B2 2.026(7), Ru1-Te1 2.6571(7), Ru1-B7 2.451(7), Ru1-Ru3 2.8175(7), Ru2-Ru3 2.7242(7), Ru3-Te1 2.6674(6), Te1-B3 2.397(7); B3-Co1-B7 94.2(3), B7-Co1-Te1 64.24(19).

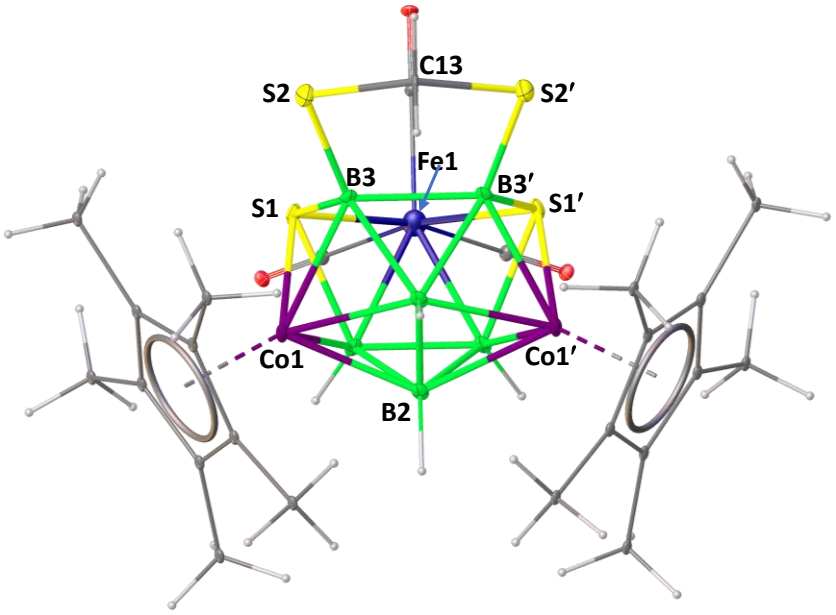

Figure S7. Molecular structure and labeling diagram of **10**. Thermal ellipsoids of core are set at the 40% probability level. One CH_2Cl_2 molecule is omitted for clarity. Selected bond lengths (Å) and angles (°): Co1-B3′ 2.072(7), Co1-B2 2.095(5), Co1′-S1′ 2.2081(17), Fe1-S1 2.3033(18), S1-B3 1.867(7), B3-B3′ 1.857(13), S2-B3 1.856(7), S2-C13 1.817(6), B3-B4 1.799(10); B4-Co1-B1 87.7(3), B3-Co1-S1 51.6(2), B4-Co1′-S1′ 92.3(3), S1-Fe1-S1′ 92.78(9), S2′-B3′-S1′ 118.4(4), S2-C13-S2′ 111.6(5).

I.2 Spectroscopic details

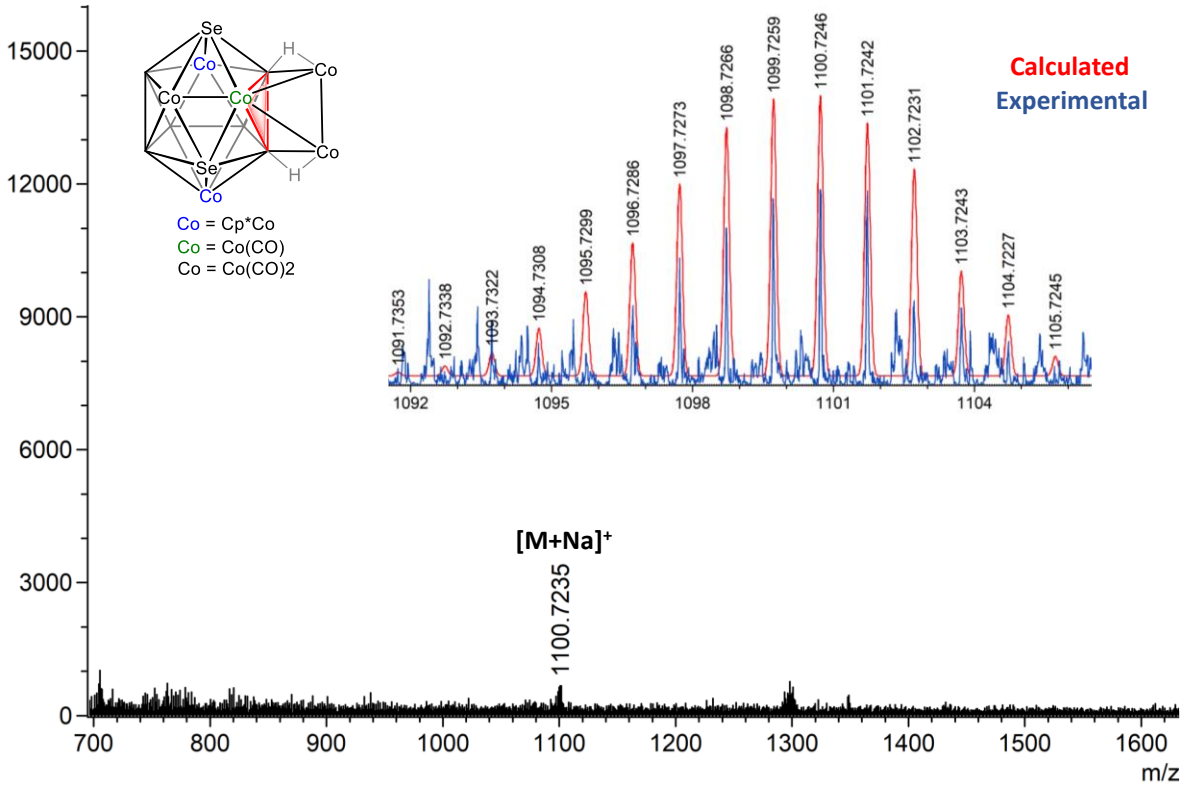

Figure S8. ESI-MS spectrum of **3** in CH_2Cl_2

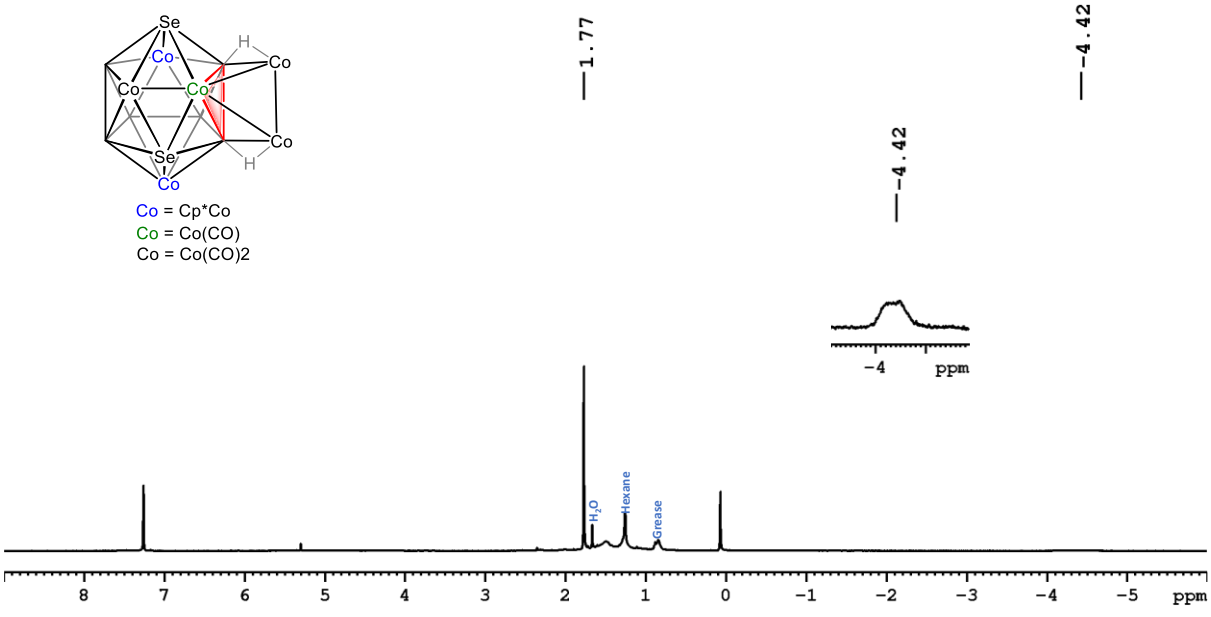

Figure S9. ^1H NMR spectrum of **3** in $CDCl_3$

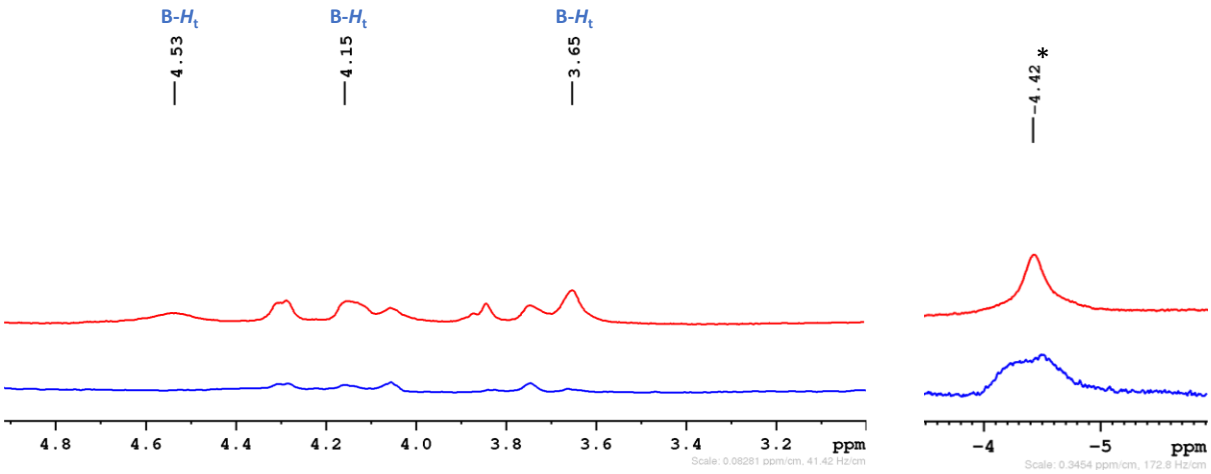

Figure S10. Stacked ^{1}H (bottom) and $^{1}H\{^{11}B\}$ NMR (top) spectrum of **3** in $CDCl_3$ (*Co-*H*-B)

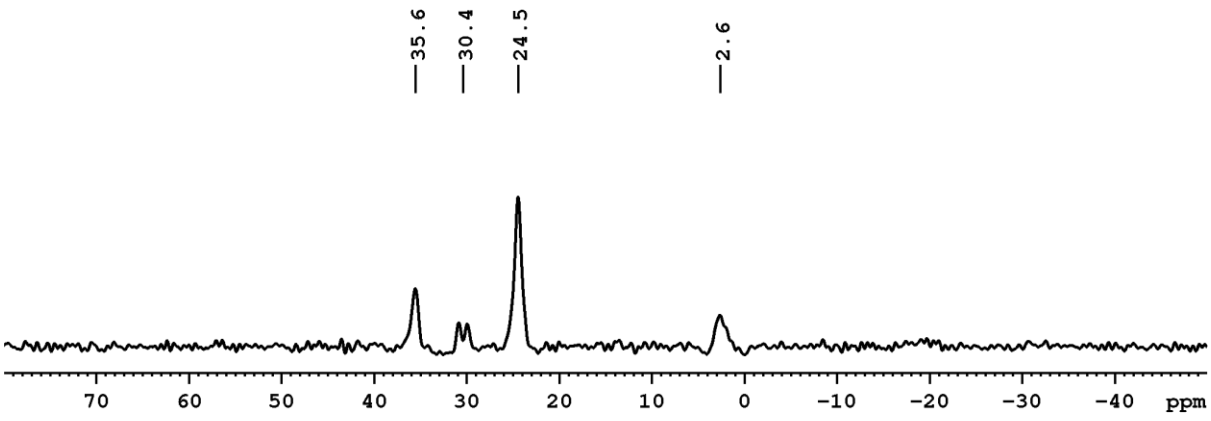

Figure S11. $^{11}B\{^{1}H\}$ NMR spectrum of **3** in $CDCl_3$[7]

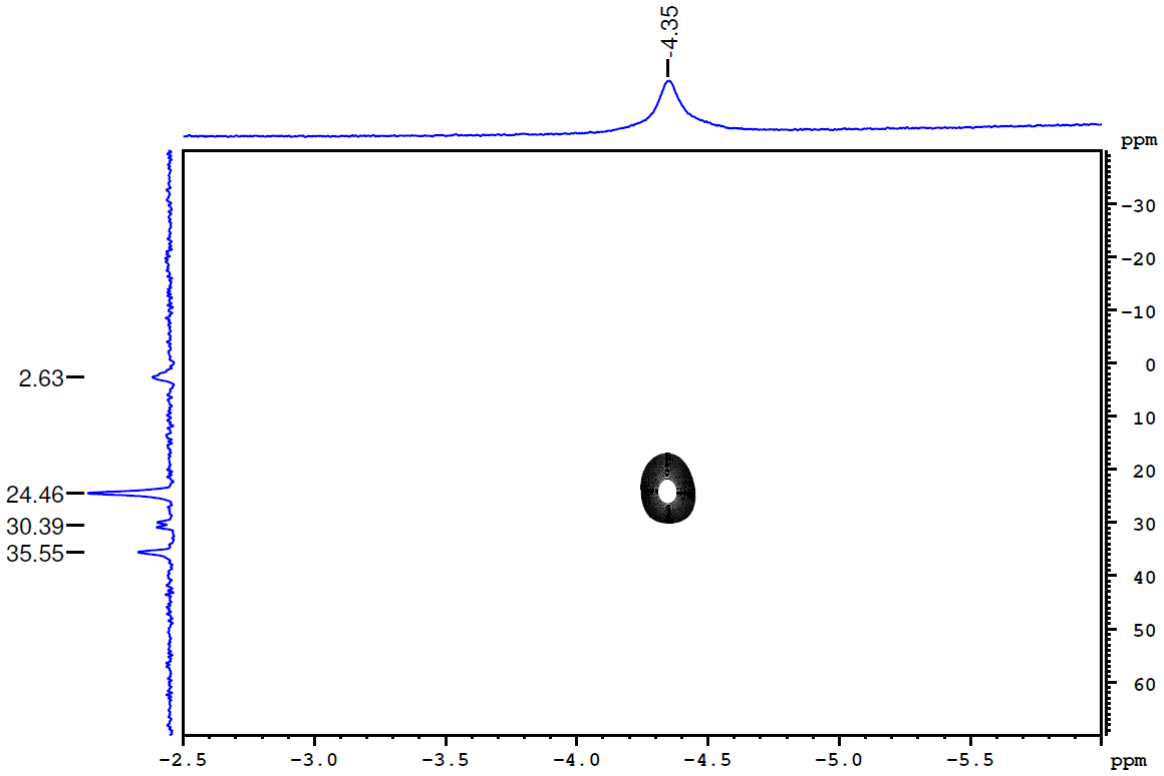

Figure S12. $^{1}H\{^{11}B\}$-$^{11}B\{^{1}H\}$ HSQC NMR spectrum of **3** in $CDCl_3$

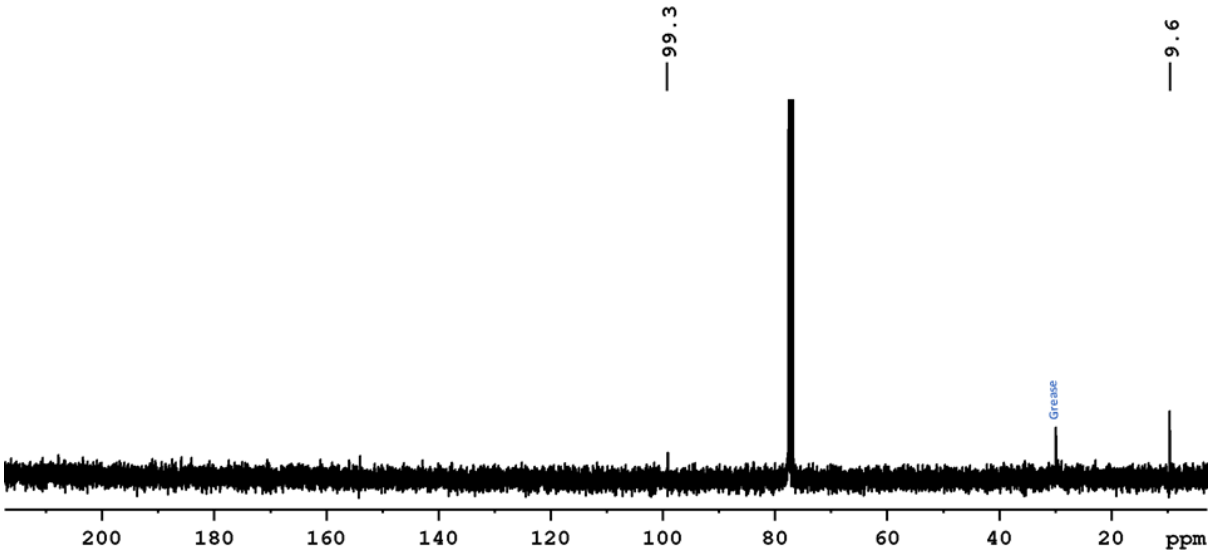

Figure S13. $^{13}C\{^{1}H\}$ NMR spectrum of **3** in $CDCl_3$

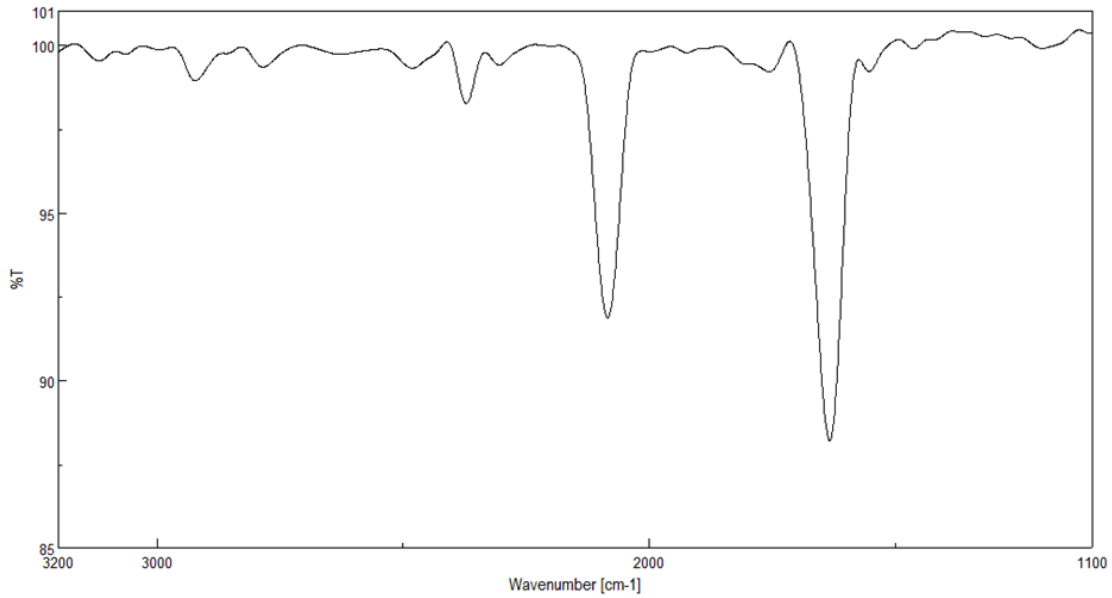

Figure S14. IR spectrum of **3** in CH_2Cl_2

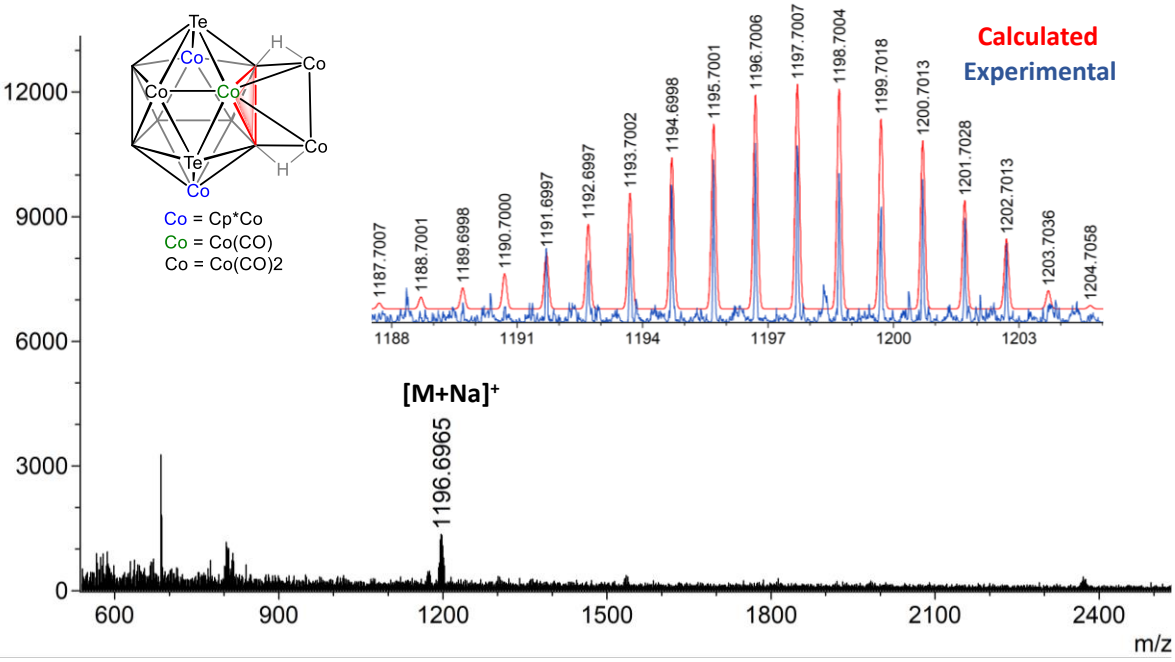

Figure S15. ESI-MS spectrum of **4** in CH_2Cl_2

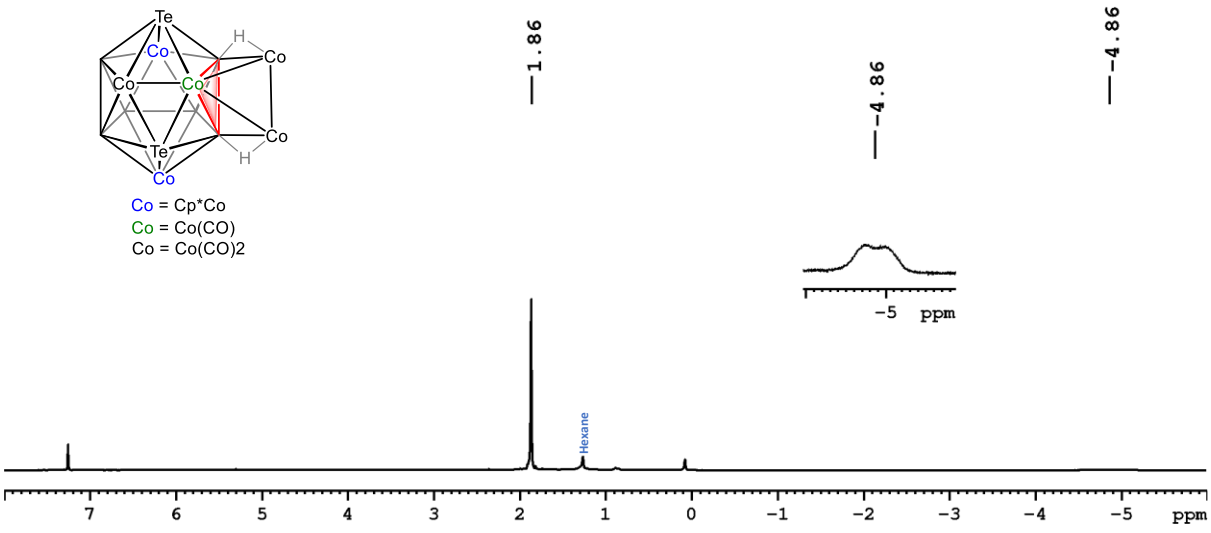

Figure S16. ^{1}H NMR spectrum of **4** in $CDCl_3$

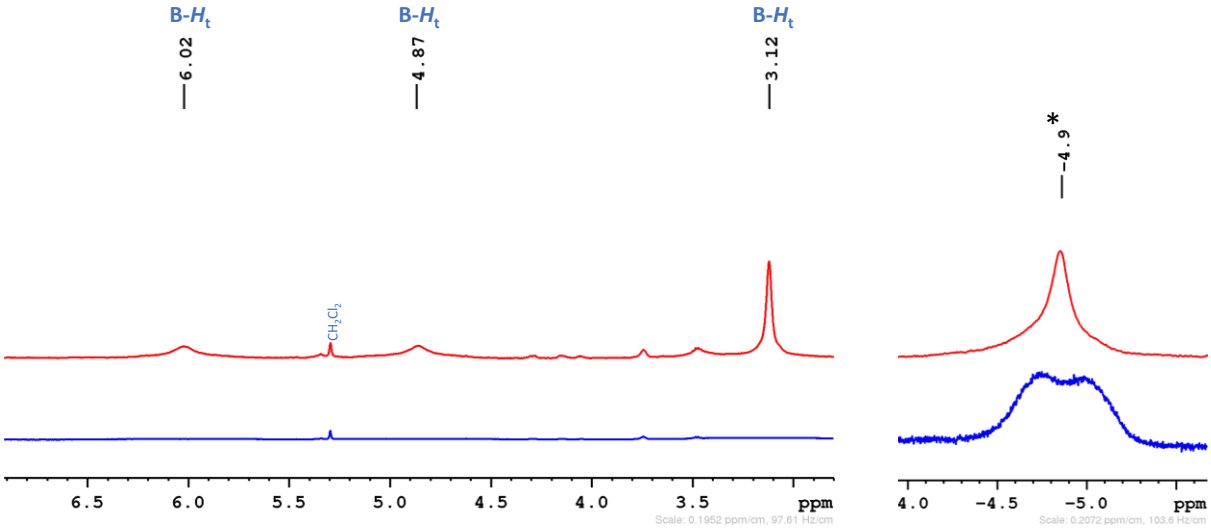

Figure S17. Stacked ^{1}H (bottom) and ^{1}H{^{11}B} NMR (top) spectrum of **4** in $CDCl_3$ (*Co-*H*-B)

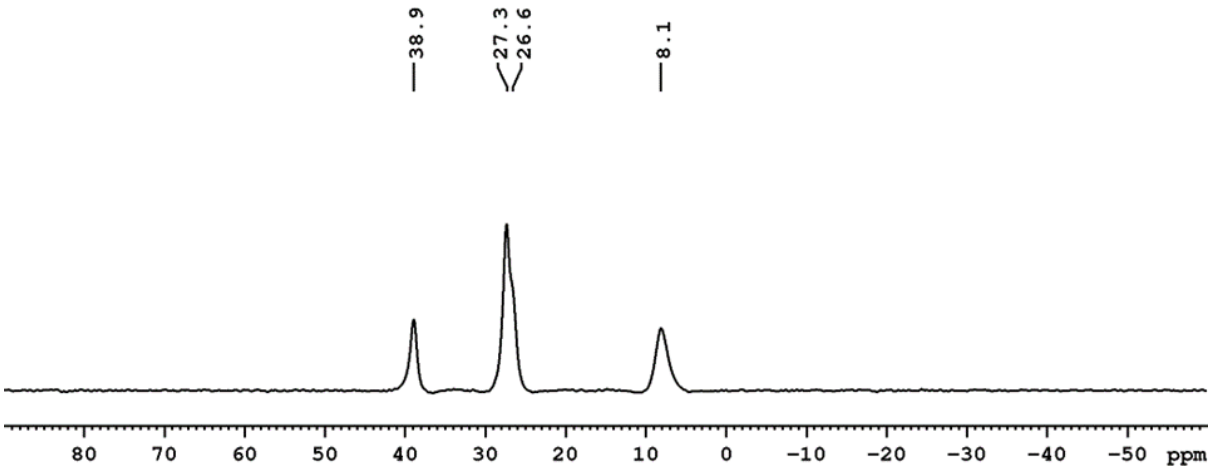

Figure S18. $^{11}B\{^{1}H\}$ NMR spectrum of **4** in $CDCl_3$[7]

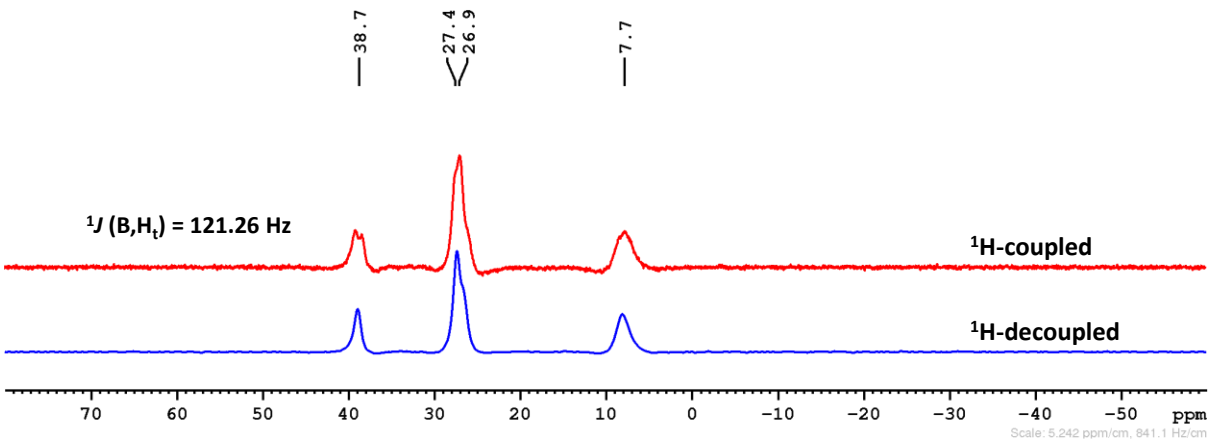

Figure S19. Stacked plot of ^{11}B (red) and $^{11}B\{^{1}H\}$ (blue) NMR spectrum of **4** in $CDCl_3$[7]

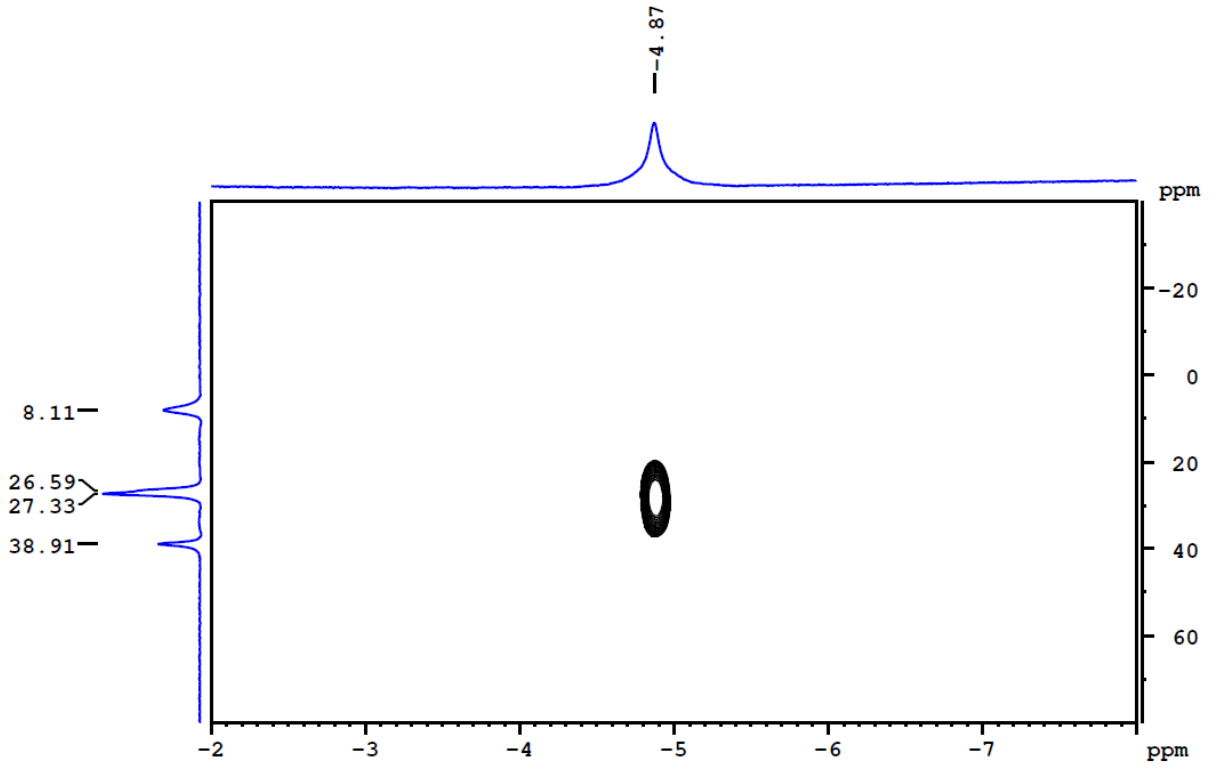

Figure S20. $^{1}H\{^{11}B\}$-$^{11}B\{^{1}H\}$ HSQC NMR spectrum of **4** in $CDCl_3$

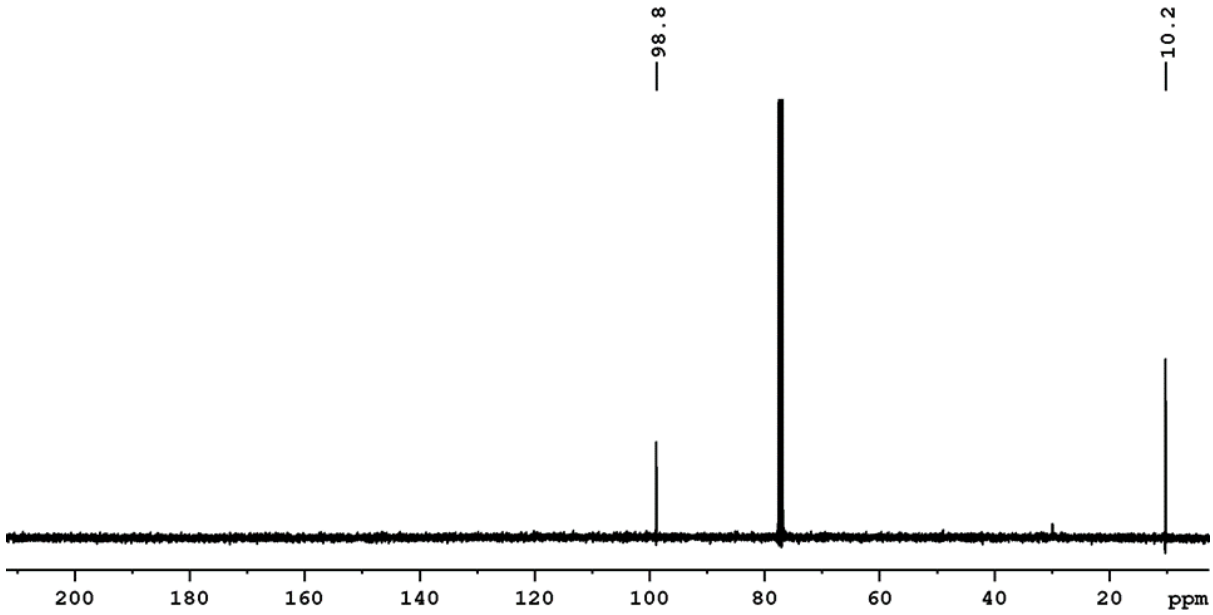

Figure S21. $^{13}C\{^{1}H\}$ NMR spectrum of **4** in $CDCl_3$

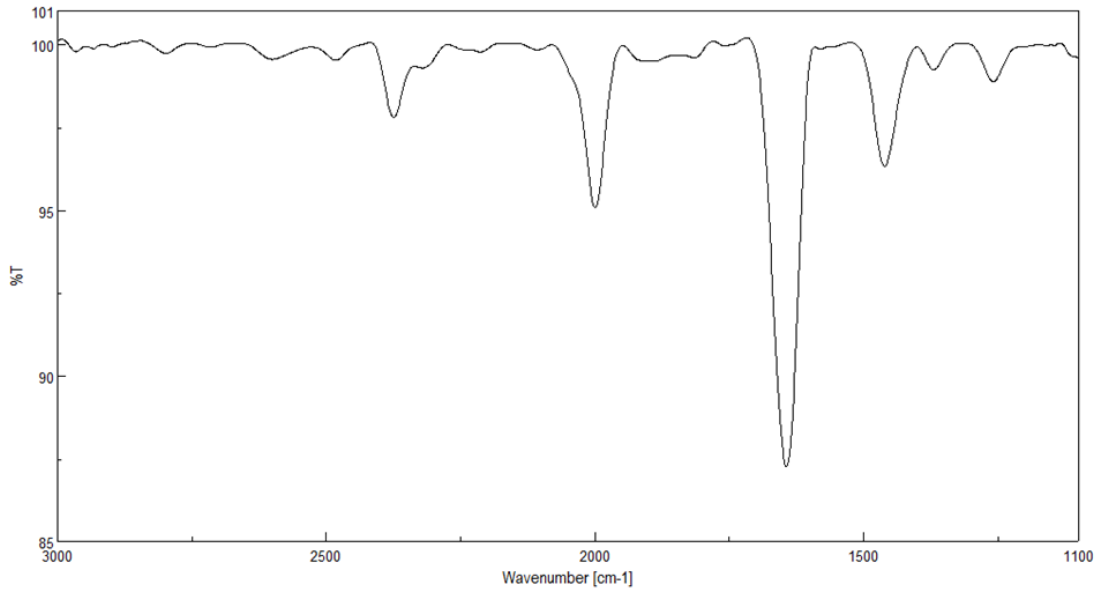

Figure S22. IR spectrum of **4** in CH_2Cl_2

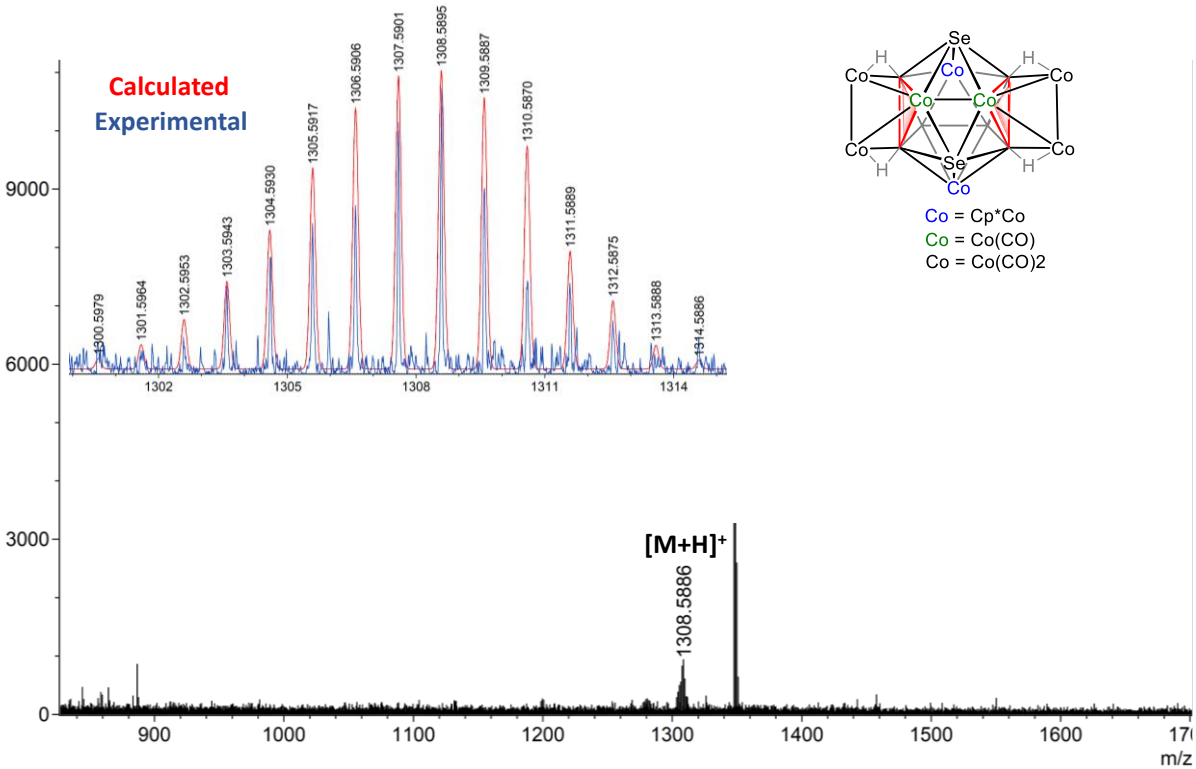

Figure S23. ESI-MS spectrum of **5** in CH_2Cl_2

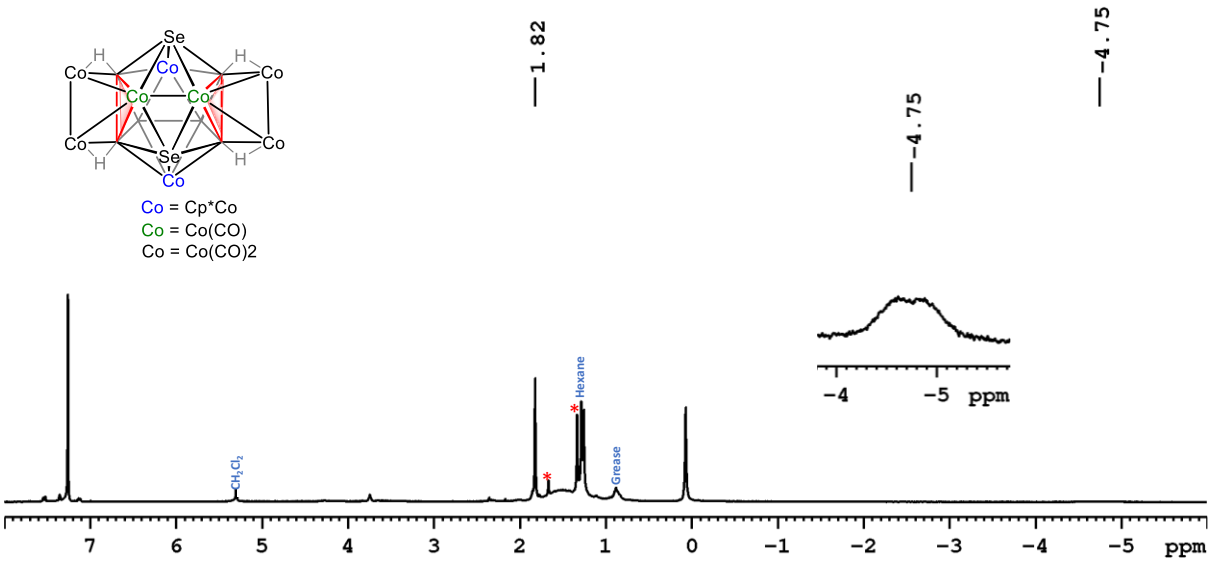

Figure S24. ^{1}H NMR spectrum of **5** in $CDCl_3$ (*inseparable impurities)

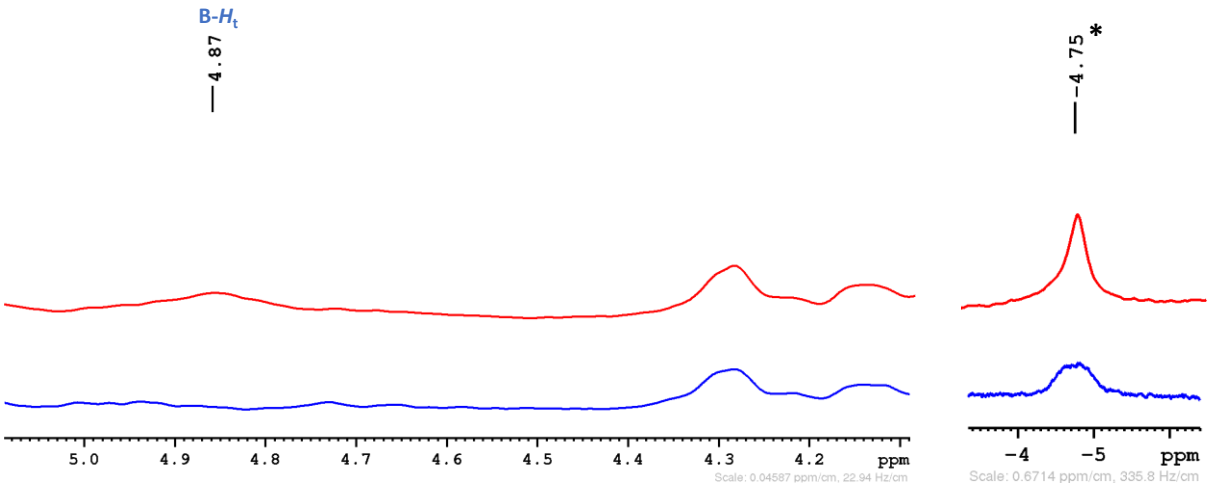

Figure S25. Stacked ^{1}H (bottom) and ^{1}H{^{11}B} NMR (top) spectrum of **5** (*Co-*H*-B)

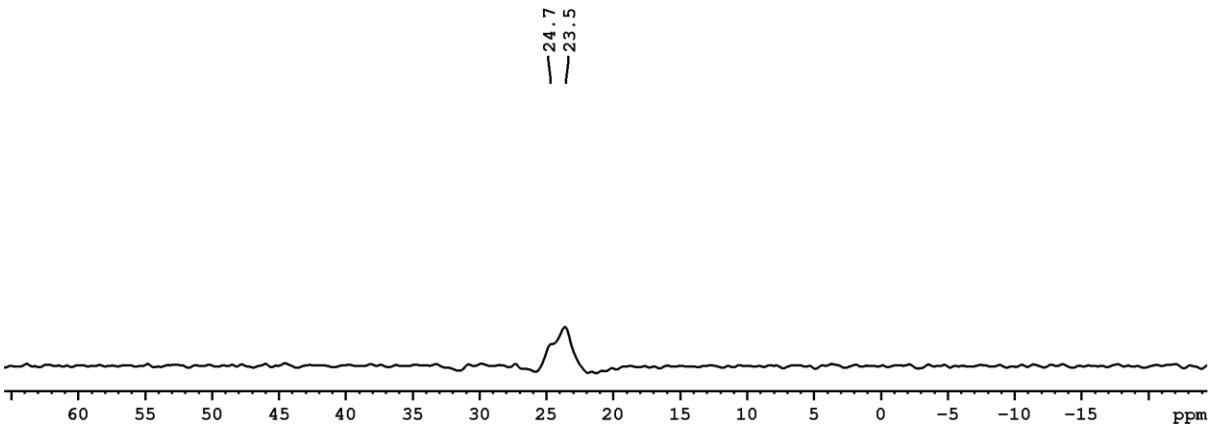

Figure S26. $^{11}B\{^{1}H\}$ NMR spectrum of **5** in $CDCl_3$[7]

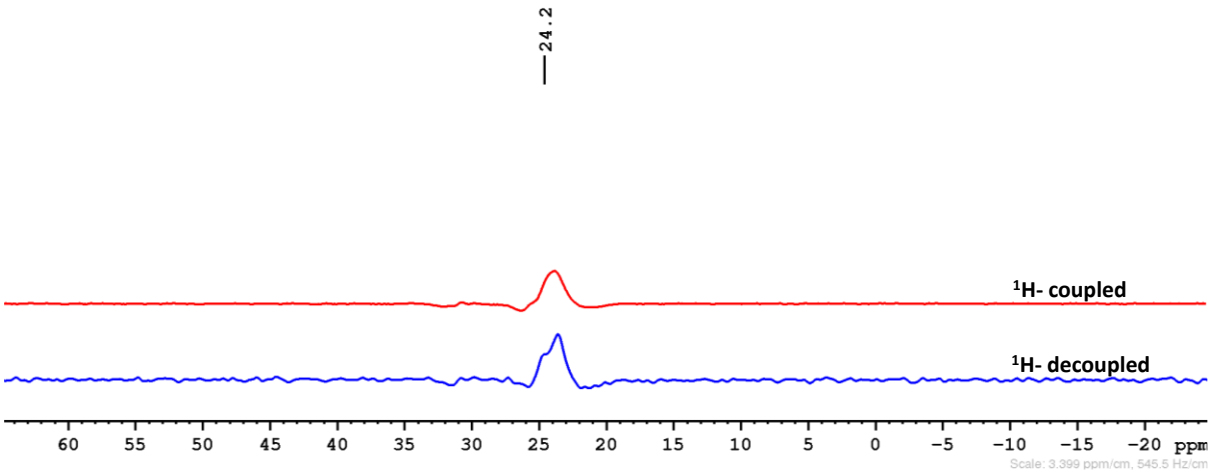

Figure S27. Stacked plot of ^{11}B (red) and $^{11}B\{^{1}H\}$ (blue) NMR spectrum of **5** in $CDCl_3$[7]

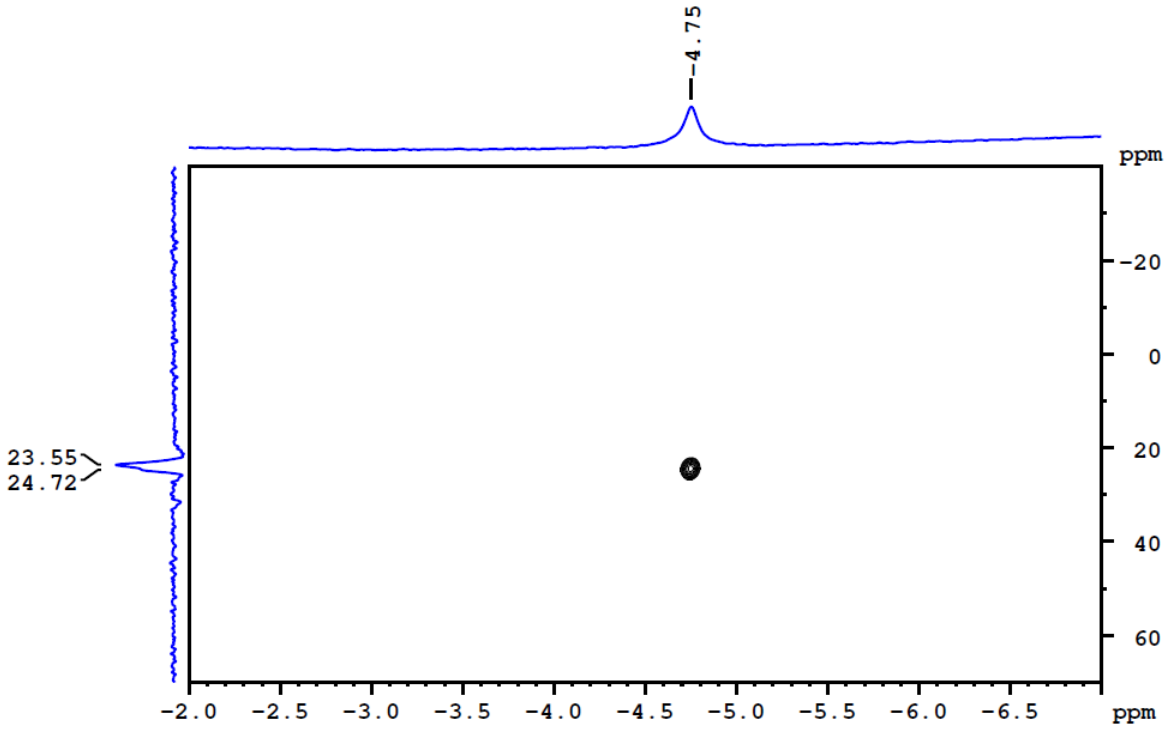

Figure S28. $^{1}H\{^{11}B\}$-$^{11}B\{^{1}H\}$ HSQC NMR spectrum of **5** in $CDCl_3$

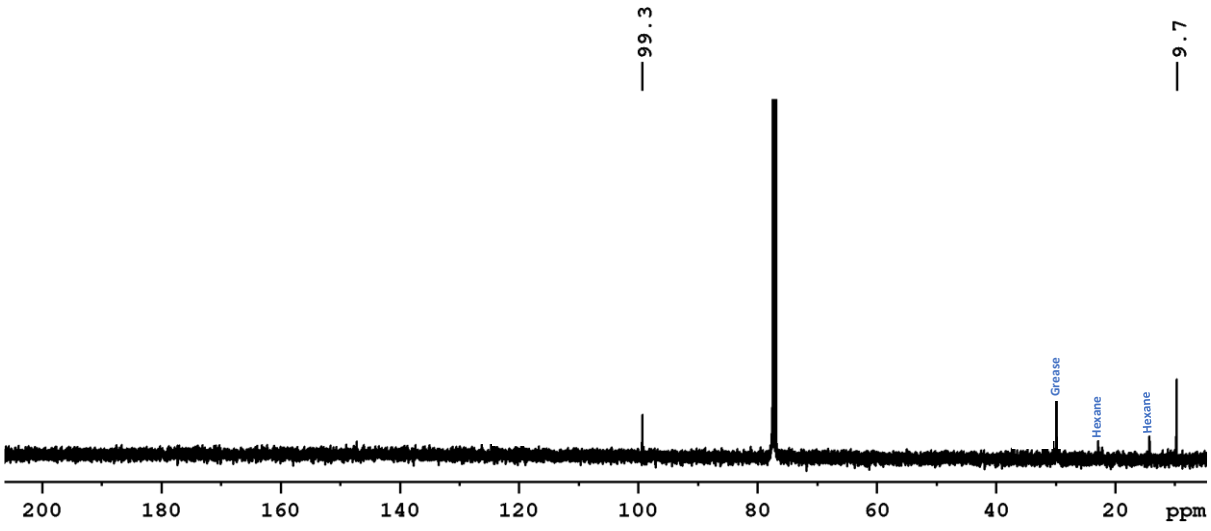

Figure S29. $^{13}C\{^{1}H\}$ NMR spectrum of **5** in $CDCl_3$

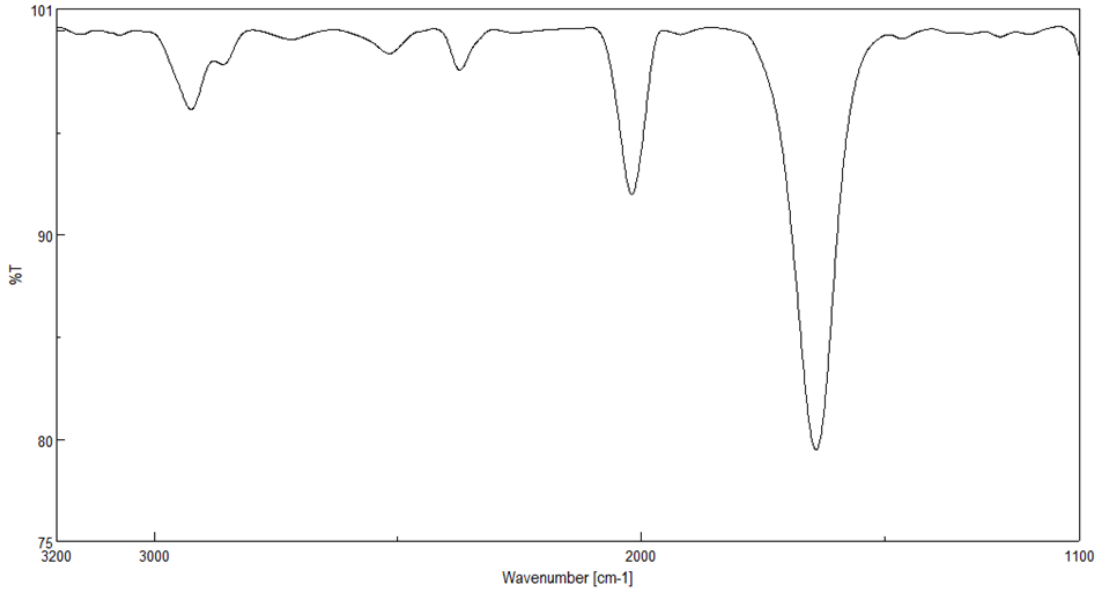

Figure S30. IR spectrum of **5** in CH_2Cl_2

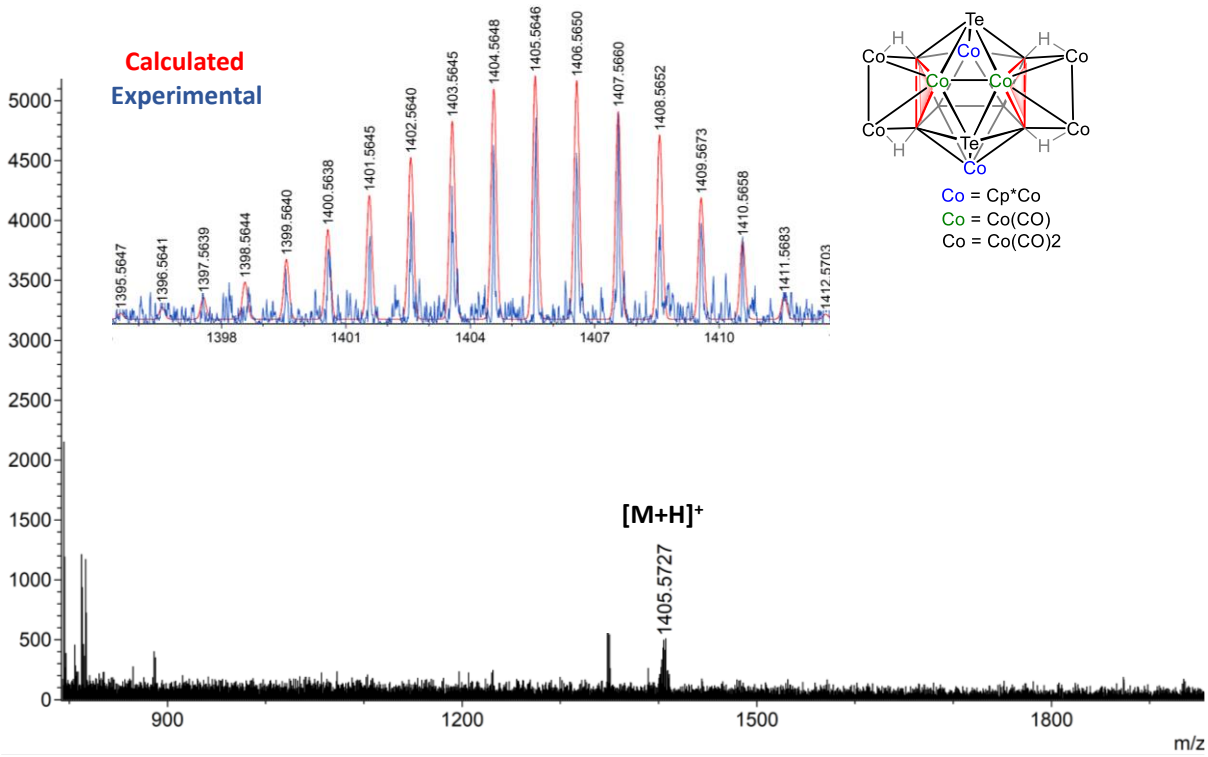

Figure S31. ESI-MS spectrum of **6** in CH_2Cl_2

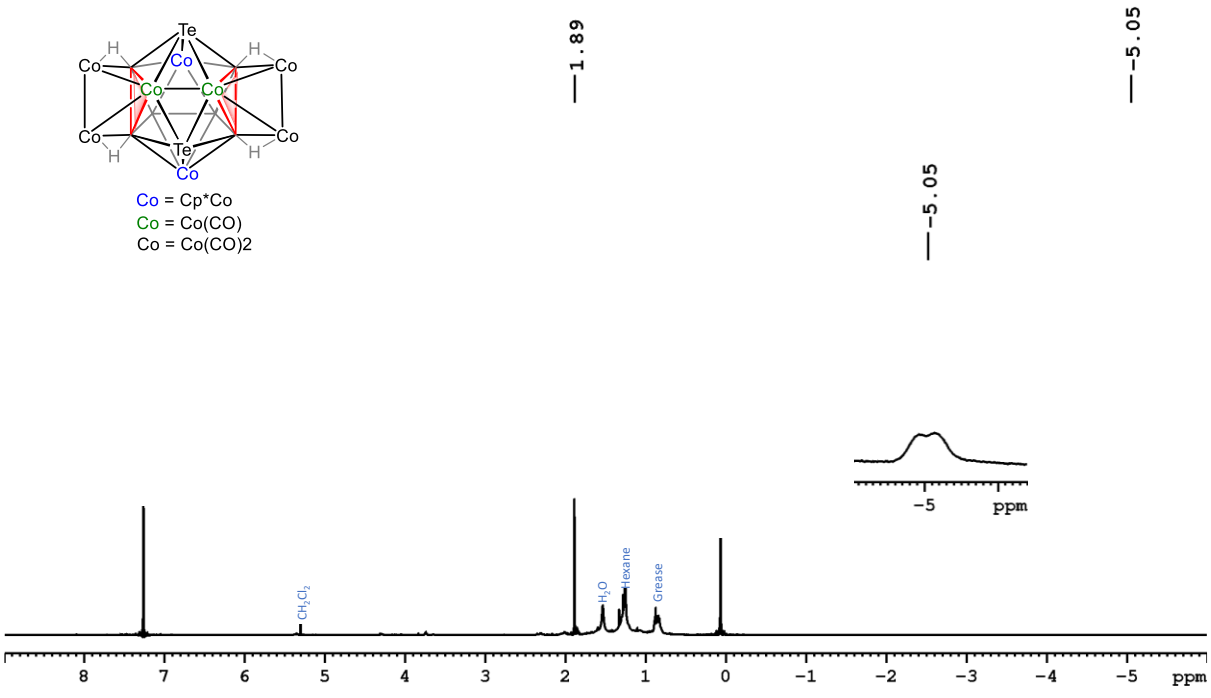

Figure S32. ^{1}H NMR spectrum of **6** in $CDCl_3$

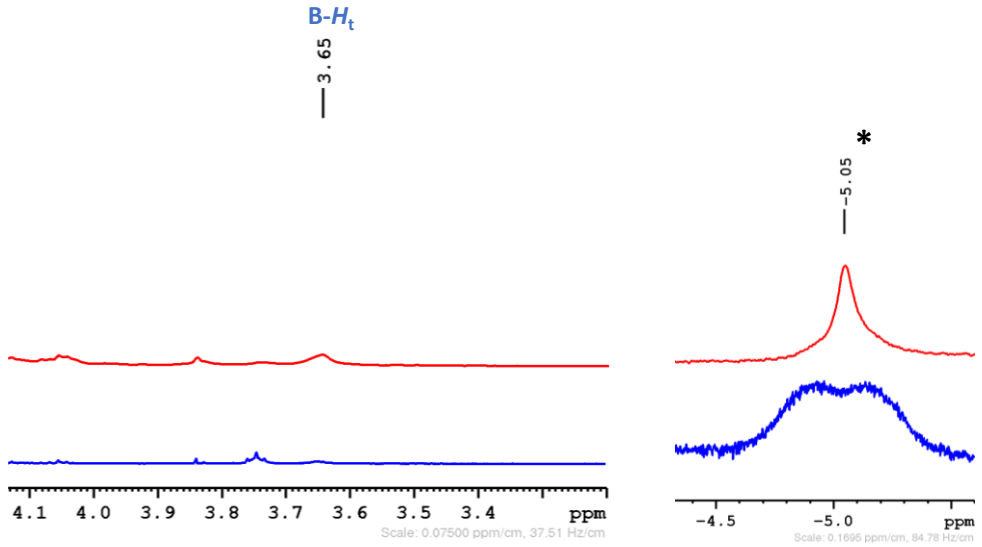

Figure S33. Stacked ^{1}H (bottom) and ^{1}H{^{11}B} NMR (top) spectrum of **6** in $CDCl_3$(*Co-*H*-B)

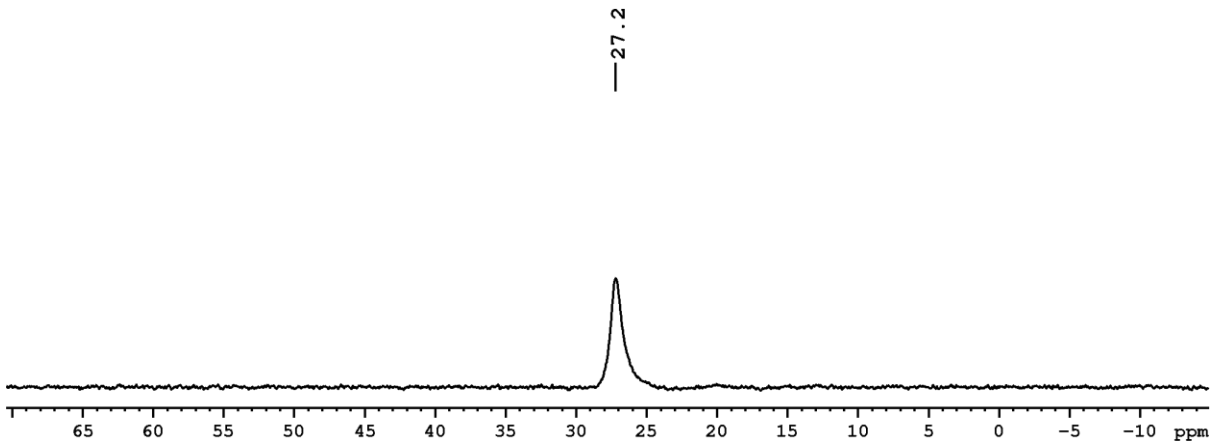

Figure S34. $^{11}B\{^{1}H\}$ NMR spectrum of **6** in $CDCl_3$[7]

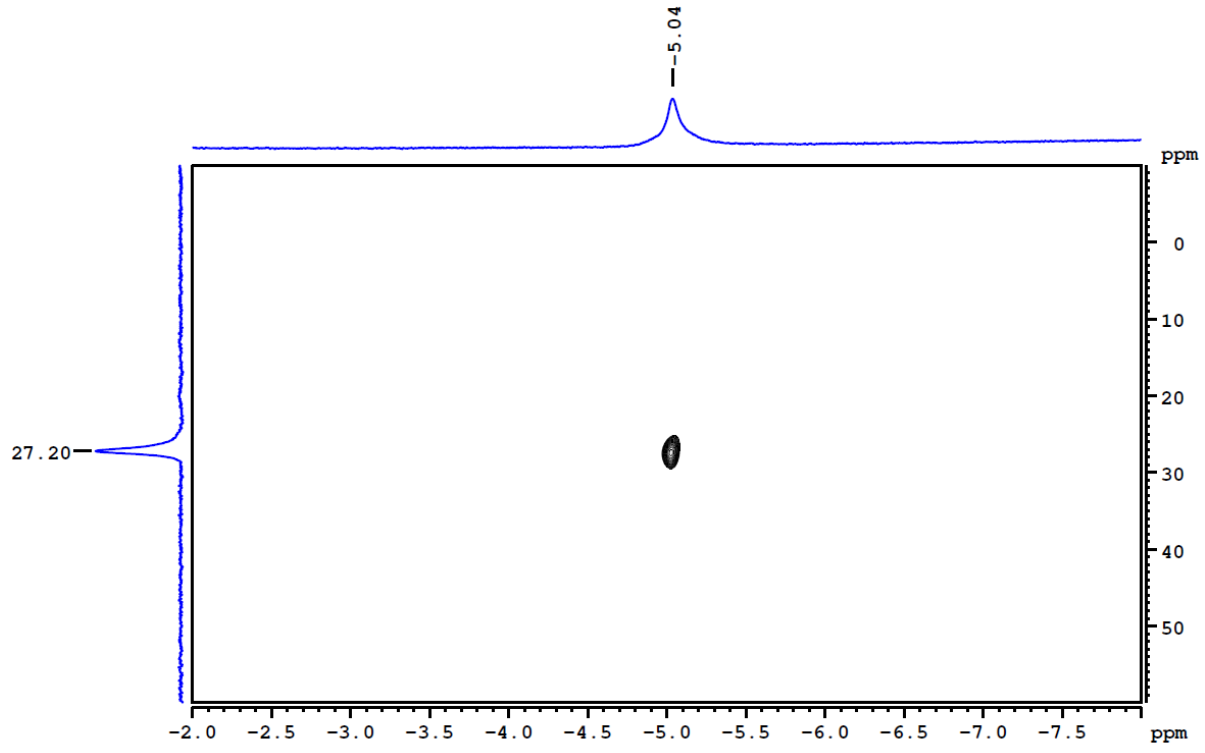

Figure S35. $^{1}H\{^{11}B\}$-$^{11}B\{^{1}H\}$ HSQC NMR spectrum of **6** in $CDCl_3$

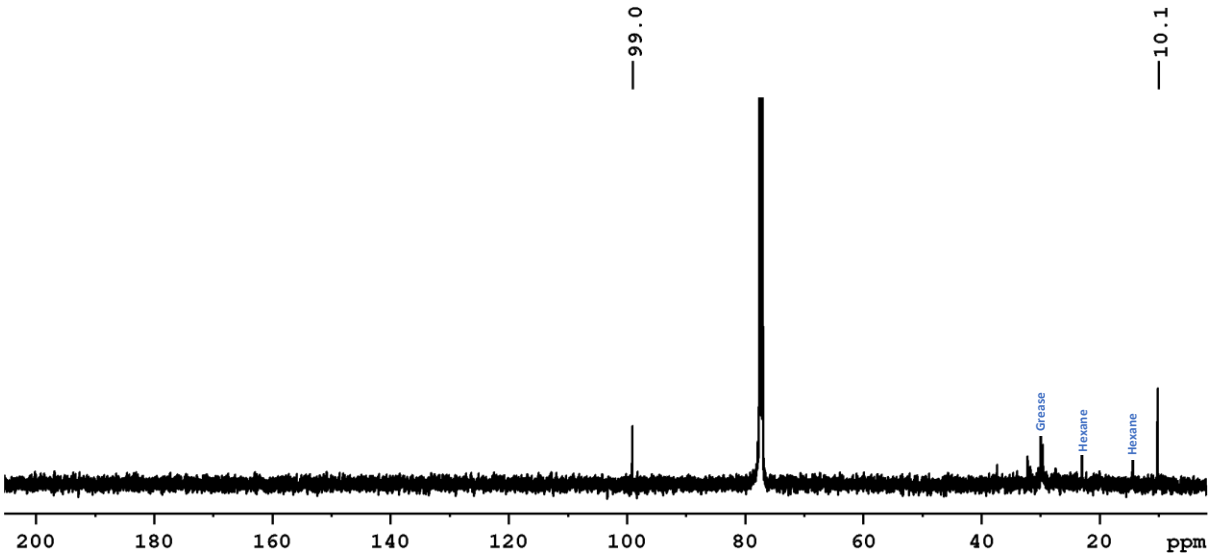

Figure S36. $^{13}C\{^{1}H\}$ NMR spectrum of **6** in $CDCl_3$

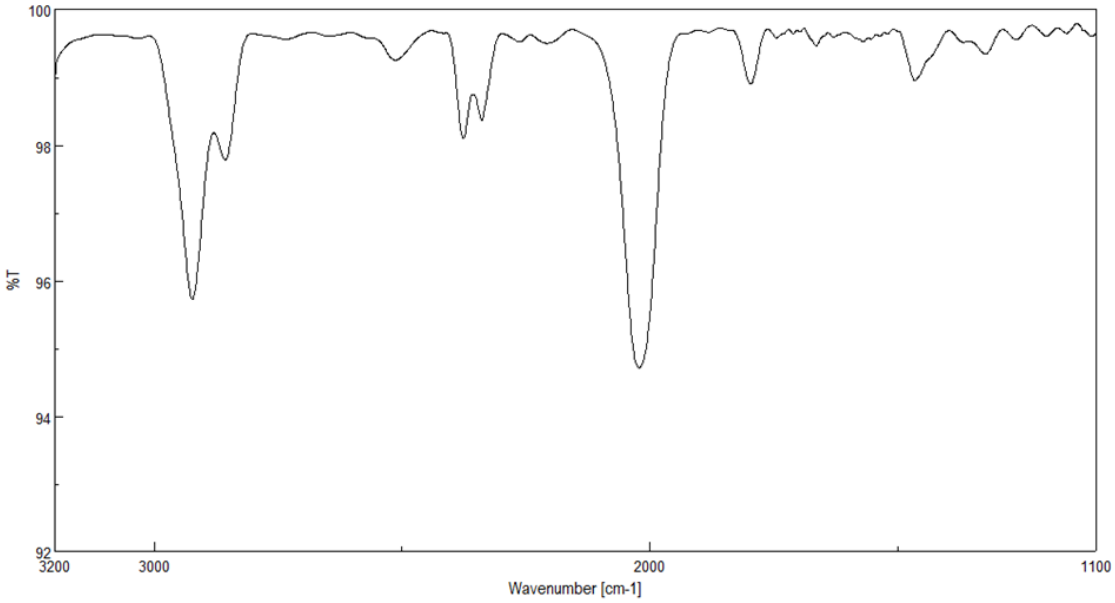

Figure S37. IR spectrum of **6** in CH_2Cl_2

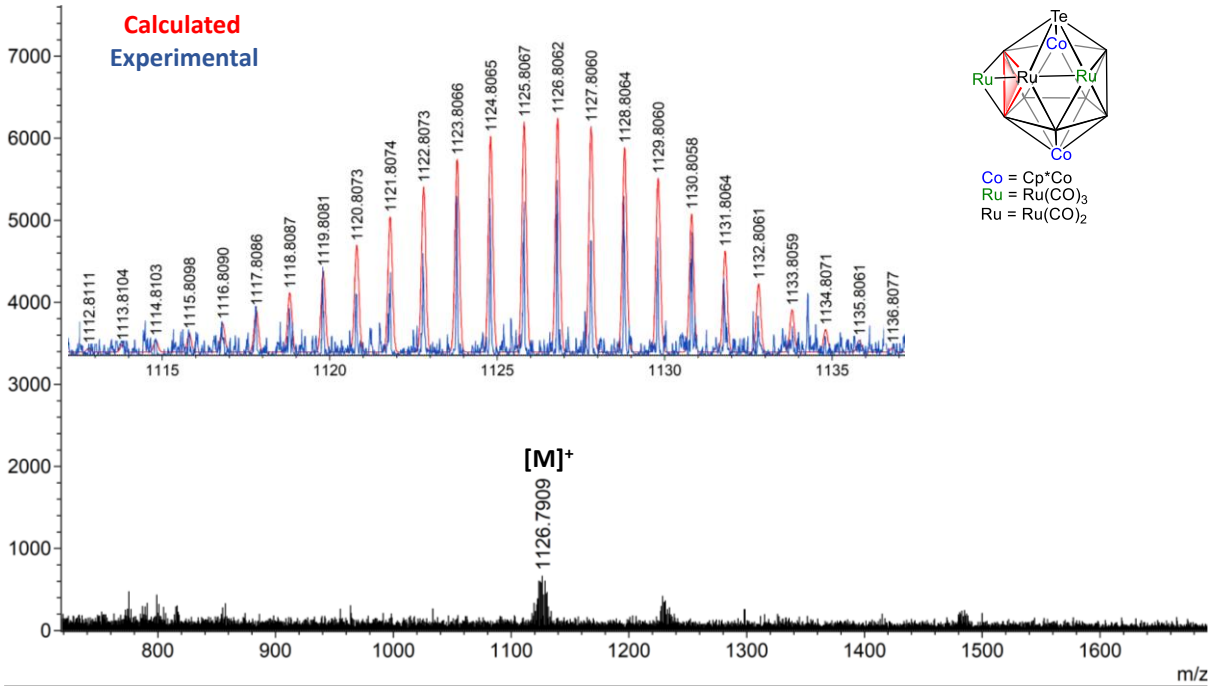

Figure S38. ESI-MS spectrum of **8** in CH_2Cl_2

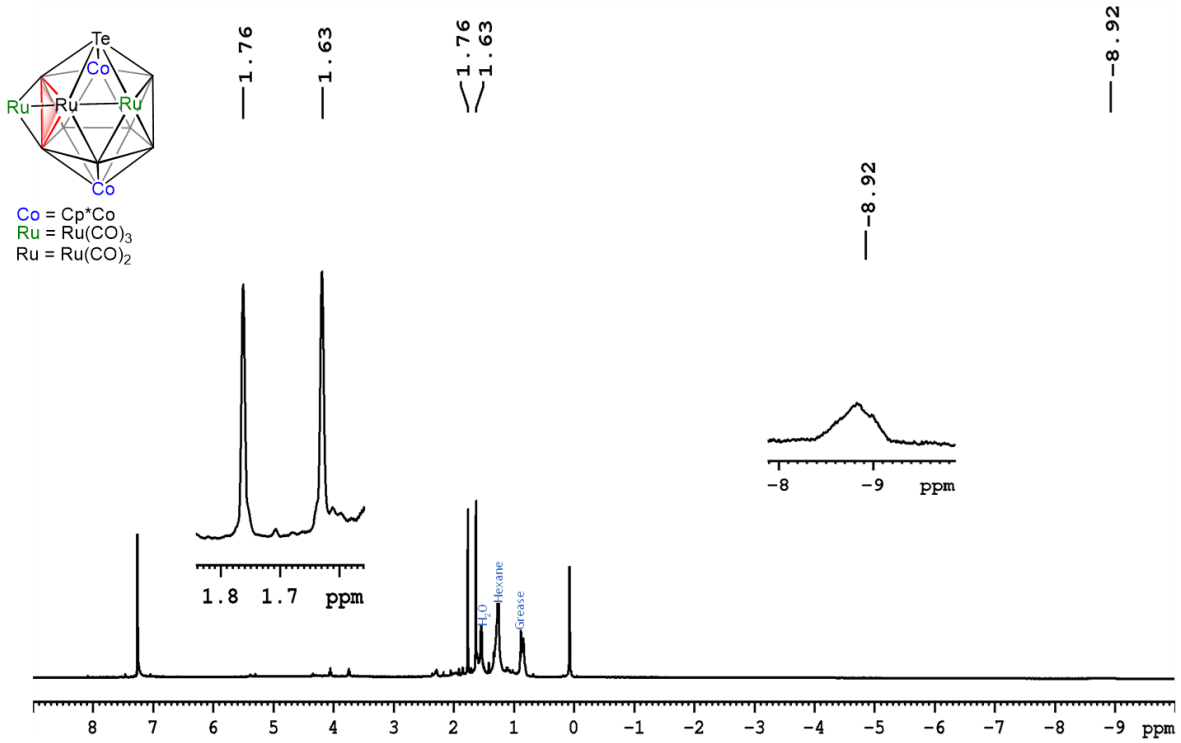

Figure S39. ^{1}H NMR spectrum of **8** in $CDCl_3$

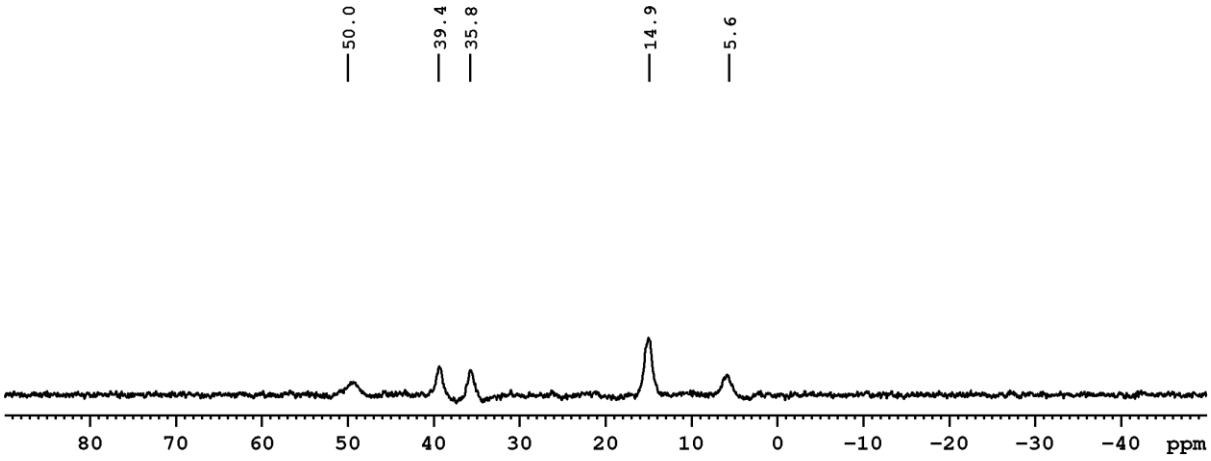

Figure S40. $^{11}B\{^{1}H\}$ NMR spectrum of **8** in $CDCl_3$[7]

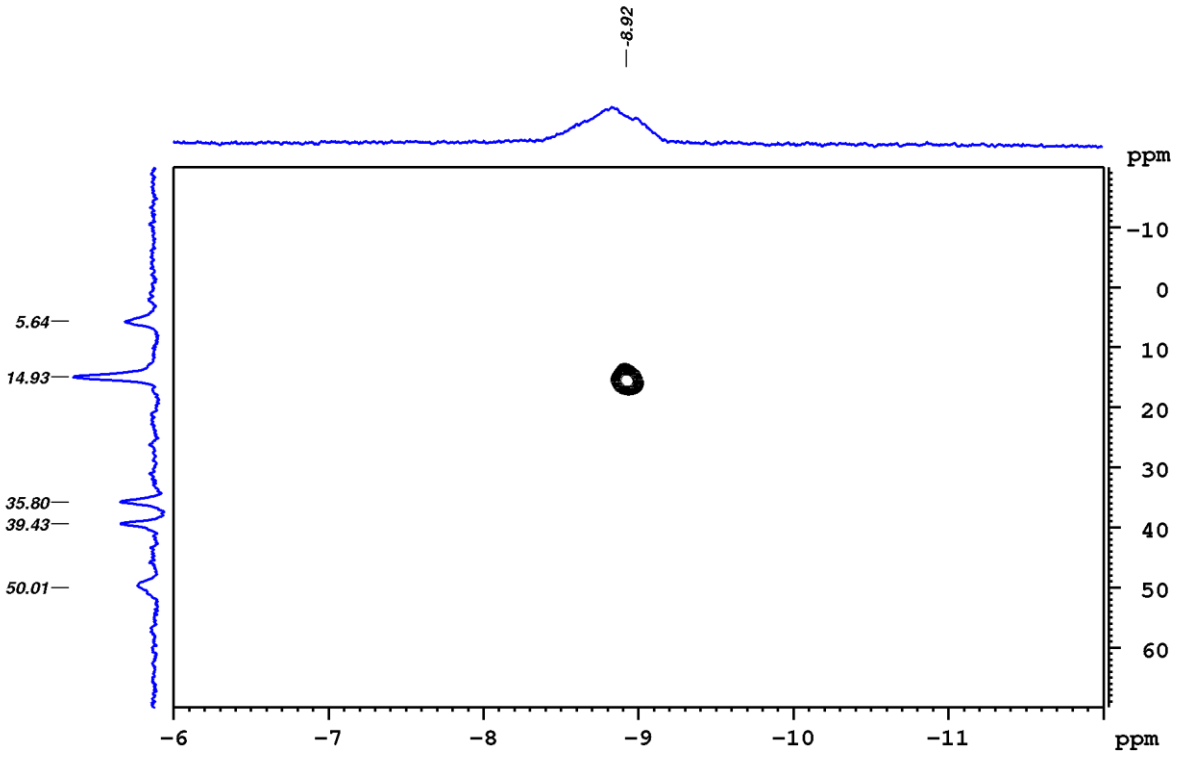

Figure S41. ^{1}H-$^{11}B\{^{1}H\}$ HSQC NMR spectrum of **8** in $CDCl_3$

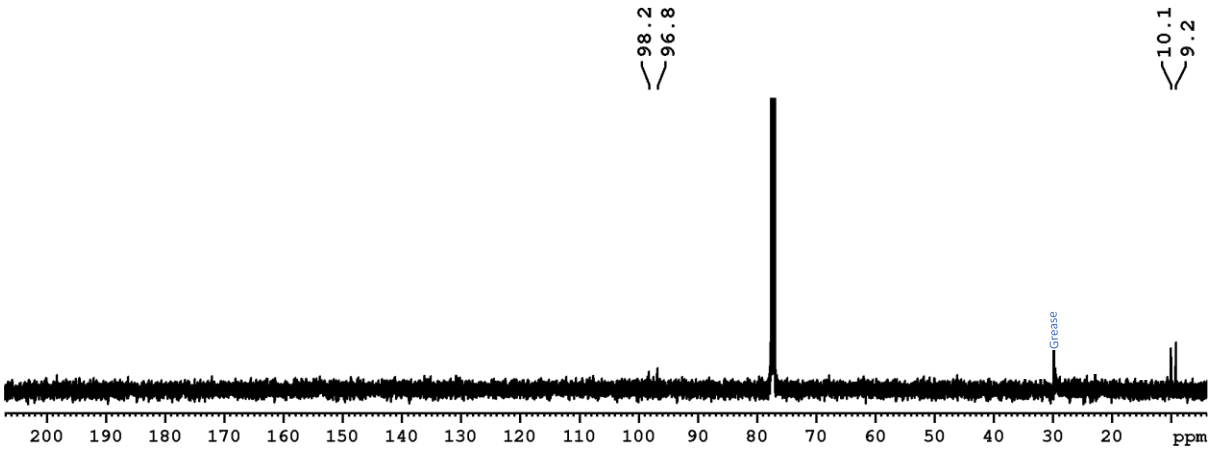

Figure S42. $^{13}C\{^{1}H\}$ NMR spectrum of **8** in $CDCl_3$

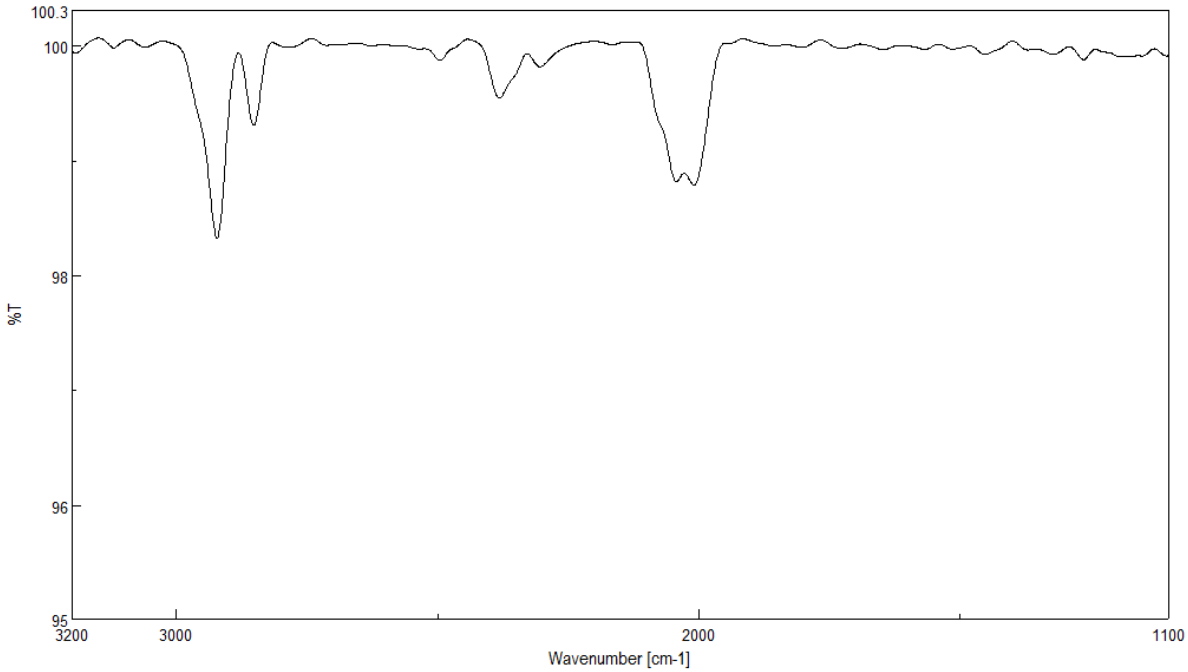

Figure S43. IR spectrum of **8** in CH_2Cl_2

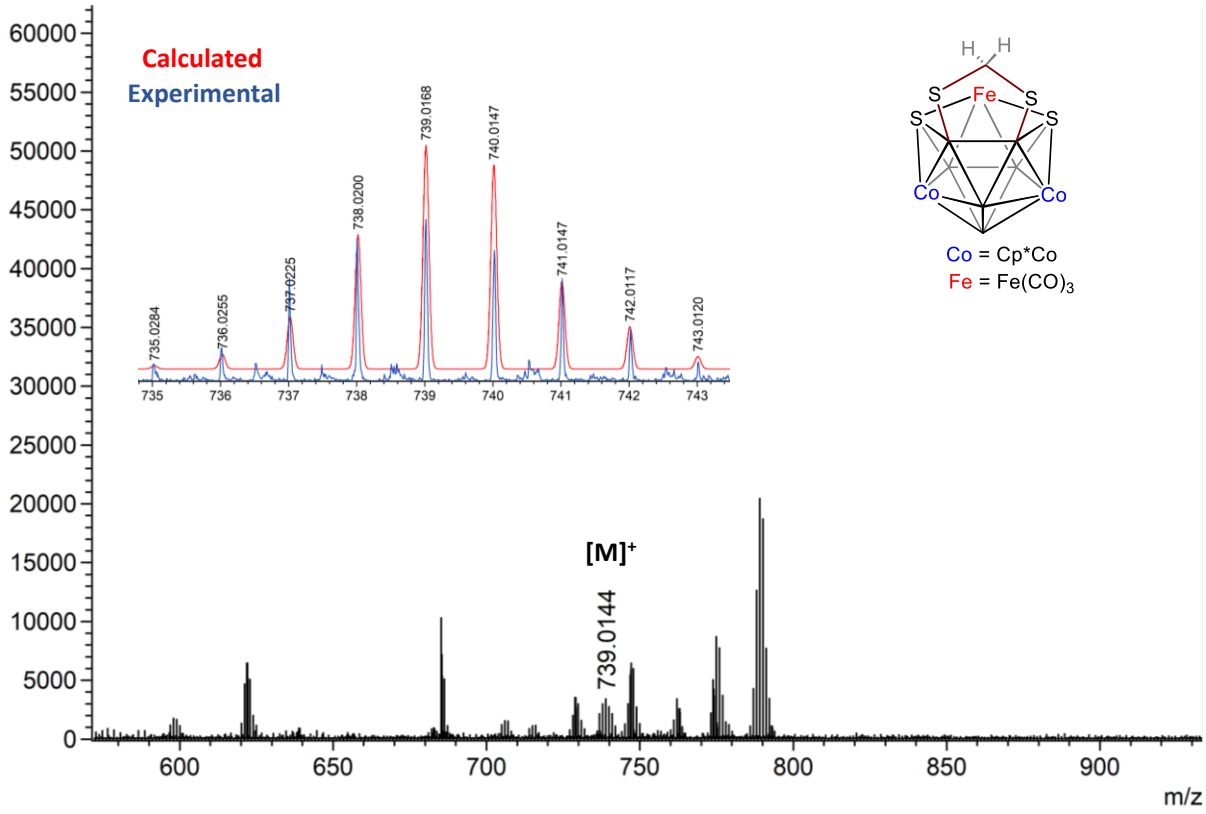

Figure S44. ESI-MS spectrum of **10** in CH_2Cl_2

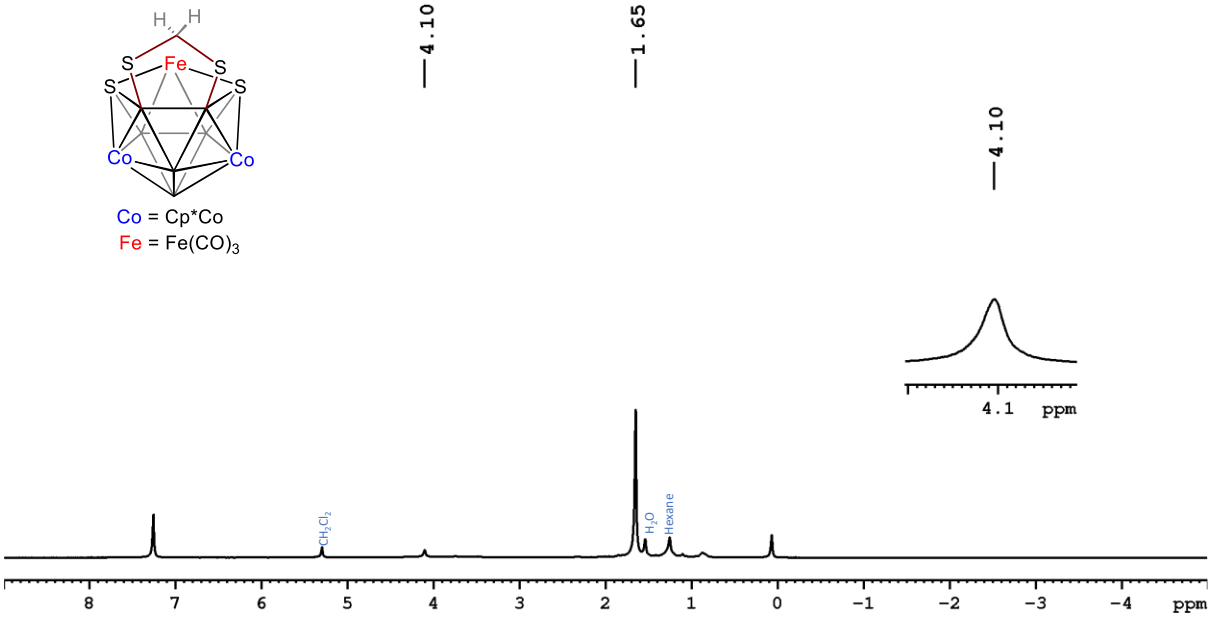

Figure S45. ^{1}H NMR spectrum of **10** in $CDCl_3$

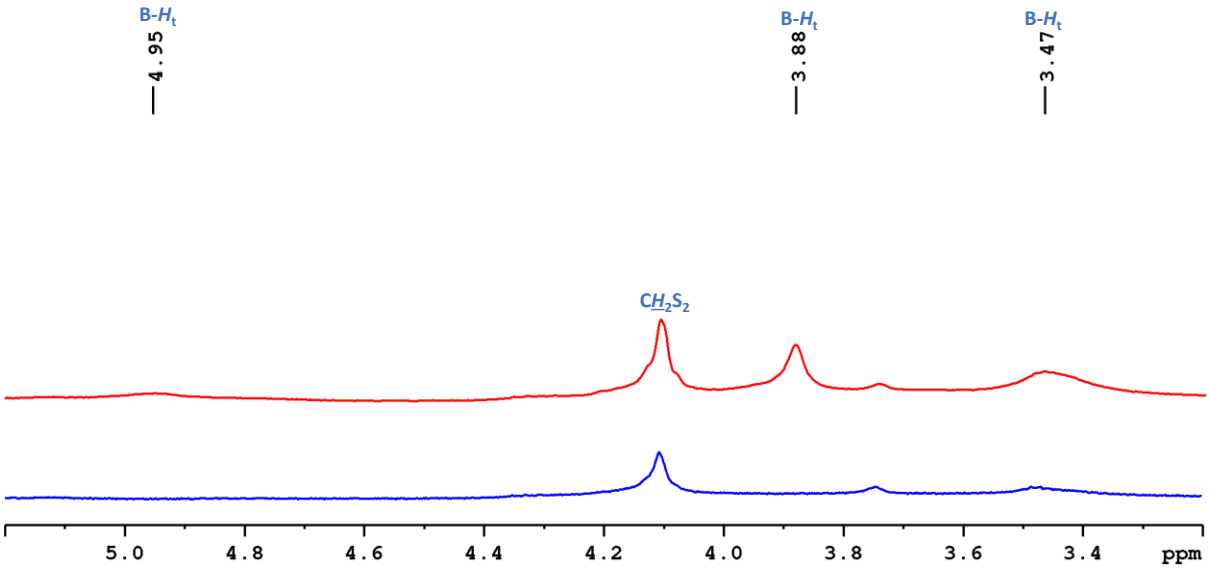

Figure S46. Stacked ^{1}H (bottom) and $^{1}H\{^{11}B\}$ NMR (top) spectrum of **10** in $CDCl_3$

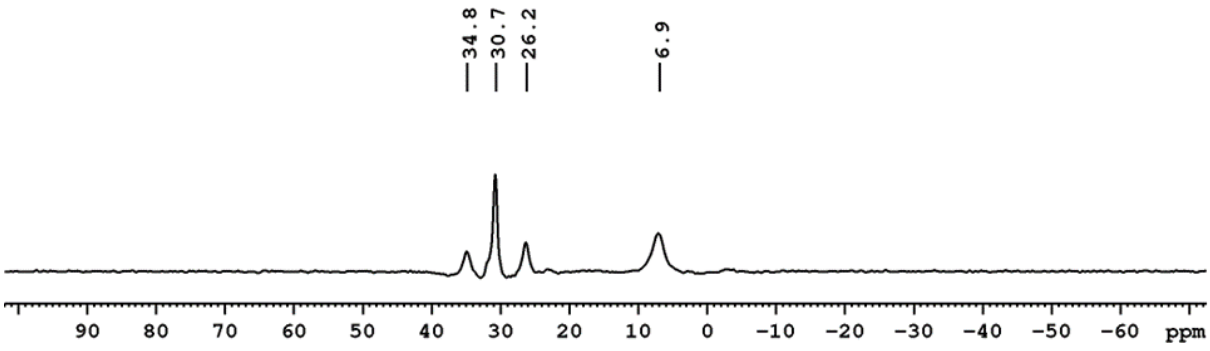

Figure S47. $^{11}B\{^{1}H\}$ NMR spectrum of **10** in $CDCl_3$[7]

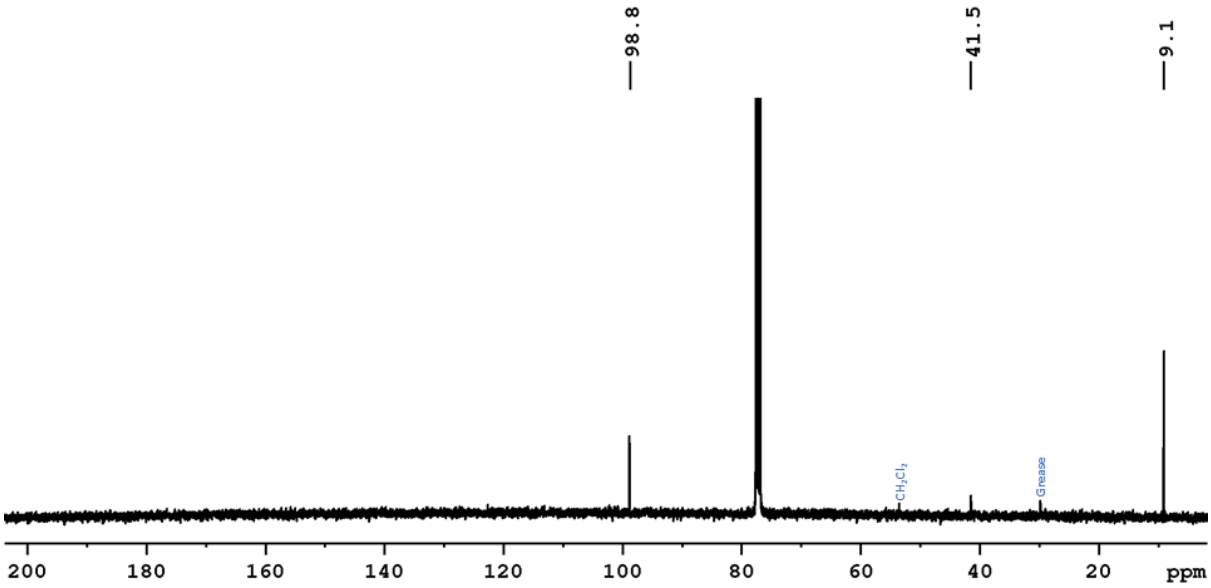

Figure S48. $^{13}C\{^{1}H\}$ NMR spectrum of **10** in $CDCl_3$

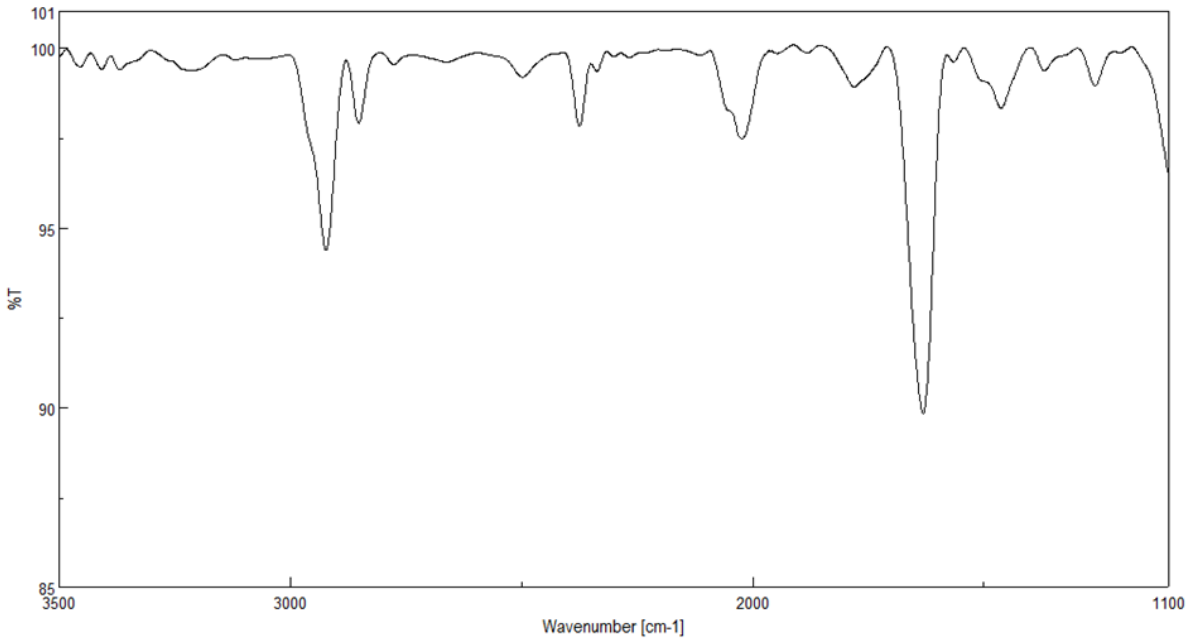

Figure S49. IR spectrum of **10** in CH_2Cl_2

II Computational Details: Optimizations of clusters are done using the Gaussian 16 program.[8] The gradient-corrected B3LYP[9] functional along with def2-TZVP basis set from EMSL[10] Basis Set Exchange Library had been employed for the optimization. Starting from X-ray crystallographic coordinates, the model compounds were fully optimized without any solvent effect in the gaseous state. The calculations were performed with the Cp analogs instead of Cp* for clusters **3**-**6** and **8** to reduce computational effort. Frequency calculations were carried out for verification of the nature of the stationary state and to confirm the absence of any imaginary frequency, which eventually confirmed the minima on the potential energy hypersurface for all structures. NMR chemical shifts were computed by employing the gauge-including atomic orbitals (GIAOs) method[11] using the optimized geometries at the B3LYP/def2-TZVP level. Chemical shifts corresponding to ^{11}B NMR were computed in relation to B_2H_6 (B3LYP shielding constant for ^{11}B NMR: 89.3 ppm) and were then converted to the standard [$BF_3{\cdot}OEt_2$] scale by adding 16.6 ppm (the experimental δ (^{11}B) value of B_2H_6) to the computed values.[12] Wiberg bond indices (WBI)[13] were obtained from natural bond orbital analysis (NBO)[14]. All the optimized structures and orbital pictures were created with the Chemcraft[15] visualization program. Two-dimensional electron density and Laplacian electronic distribution plots were generated using the Multiwfn package.[16]

Table S2. Selected geometrical parameters and Wiberg indices (WBIs) of **3′-6′**, **8′**, and **10′**.

3/3′				**4/4′**			
	Expt.	Cal.	WBI		Expt.	Cal.	WBI
Co5-Se1	2.388	2.391	0.480	Co4-Te1	2.505	2.536	0.527
Co5-Co4	2.505	2.502	0.409	Co4-B1	2.126	2.103	0.425
Co3-Co4	2.435	2.435	0.402	Co3-Co4	2.747	2.798	0.352
Co5-B1	2.135	2.095	0.378	Co5-Co6	2.431	2.414	0.475
B4-B6	1.791	1.803	0.552	Te2-B6	2.434	2.447	0.532
Se1-B5	2.160	2.163	0.662	B3-B4	1.778	1.776	0.589
Co4-B1	2.229	2.287	0.266	Co1-Te2	2.474	2.524	0.509
5/5′				**6/6′**			
	Expt.	Cal.	WBI		Expt.	Cal.	WBI
Se1-B2	2.242	2.214	0.564	Co2-Co3	2.490	2.507	0.386
Se1-Co1	2.317	2.361	0.525	B2-B2	1.834	1.814	0.526
Co3-B2	2.117	2.100	0.380	Te1-B1	2.444	2.428	0.492
B1-B2	1.756	1.776	0.566	Te1-Co2	2.464	2.492	0.524
Co2-Co3	2.489	2.496	0.405	Co2-B1	2.137	2.119	0.399
Co2-Co2	2.426	2.434	0.406	B1-B2	1.756	1.763	0.589
Se1-Co3	2.338	2.362	0.499	Te1-Co1	2.466	2.518	0.523
8/8′				**10/10′**			
	Expt.	Cal.	WBI		Expt.	Cal.	WBI
Te1-Ru3	2.667	2.705	0.540	Fe1-S1	2.303	2.358	0.602
Ru2-Ru3	2.724	2.761	0.408	S1-B3	1.867	1.897	0.909
Ru2-B3	2.305	2.358	0.310	S2-B3	1.856	1.850	1.138
B2-B3	1.700	1.713	0.648	B1-B2	1.801	1.787	0.548
Co1-Te1	2.469	2.508	0.538	Co1-B2	2.095	2.099	0.404
Co2-B4	2.073	2.085	0.423	C13-S2	1.817	1.828	0.997
Te1-B3	2.397	2.418	0.535	Fe1-B1	2.248	2.258	0.347

Table S3. Selected Wiberg bond indices (WBIs) of B-H and M-H for **3′-6′**.

3/3′		**4/4′**	
	WBI		WBI
B2-H_b	0.678	B1-H_b	0.685
B5-H_t	0.945	B5-H_t	0.934
Co3-H_b	0.225	Co5-H_b	0.224
5/5′		**6/6′**	
	WBI		WBI
B2-H	0.687	B1-H_b	0.677
B1-H	0.936	B2-H_t	0.934
Co2-H	0.218	Co3-H_b	0.229

[b] bridging hydrogen; [t] terminal hydrogen

Table S4. Calculated natural charges (q) and natural valence population (pop) of selected atoms for compounds **3′**and **4′**.

3′			**4′**		
	q	pop		q	pop
Co5	-0.994	9.977	Co4	-0.547	9.563
Co6	-1.154	10.144	Co3	-0.809	9.818
B1	0.031	2.907	B6	-0.248	3.197
B2	0.031	2.907	B1	-0.248	3.197
B5	-0.087	3.035	B5	-0.205	3.164
B6	-0.085	3.034	B4	-0.205	3.164
Se1	0.731	5.230	Te1	0.818	5.161

Table S5. Topological parameters at selected bond critical points (BCPs) of **3′-6′**, **8′**, and **10′**.

Clusters	BCP	ρ(r)	H(r)	$\nabla^2\rho(r)$	ELF
3′	Co3-Co5	0.490	-0.112	0.586	0.345
	Se1-Co5	0.687	-0.187	0.146	0.263
4′	Co4-Co5	0.496	-0.176	0.313	0.363
	Te1-Co4	0.615	-0.170	0.991	0.301
5′	Co2-Co3	0.492	-0.113	0.606	0.338
	Co3-Se1	0.720	-0.207	0.153	0.268
6′	Co2-Co3	0.478	-0.108	0.602	0.329
	Co2-Te1	0.670	-0.202	0.984	0.333
8′	Ru2-Ru3	0.522	-0.132	0.576	0.363
	Te1-Ru1	0.582	-0.145	0.869	0.324
10′	Fe1-S1	0.648	-0.176	0.165	0.205
	Co1-S1	0.798	-0.258	0.198	0.241

Table S6. Calculated (DFT) energies of the HOMO and LUMO (eV) and HOMO-LUMO gaps (ΔE =E_{LUMO}-E_{HOMO}, eV) of **3′-6′**, **8′,** and **10′**.

Clusters	HOMO (eV)	LUMO (eV)	ΔE_{H-L} (eV)
3′	-5.978	-3.401	2.577
4′	-5.823	-3.323	2.500
5′	-6.112	-3.668	2.444
6′	-6.122	-3.702	2.420
8′	-5.796	-2.667	3.129
10′	-5.291	-2.418	2.873

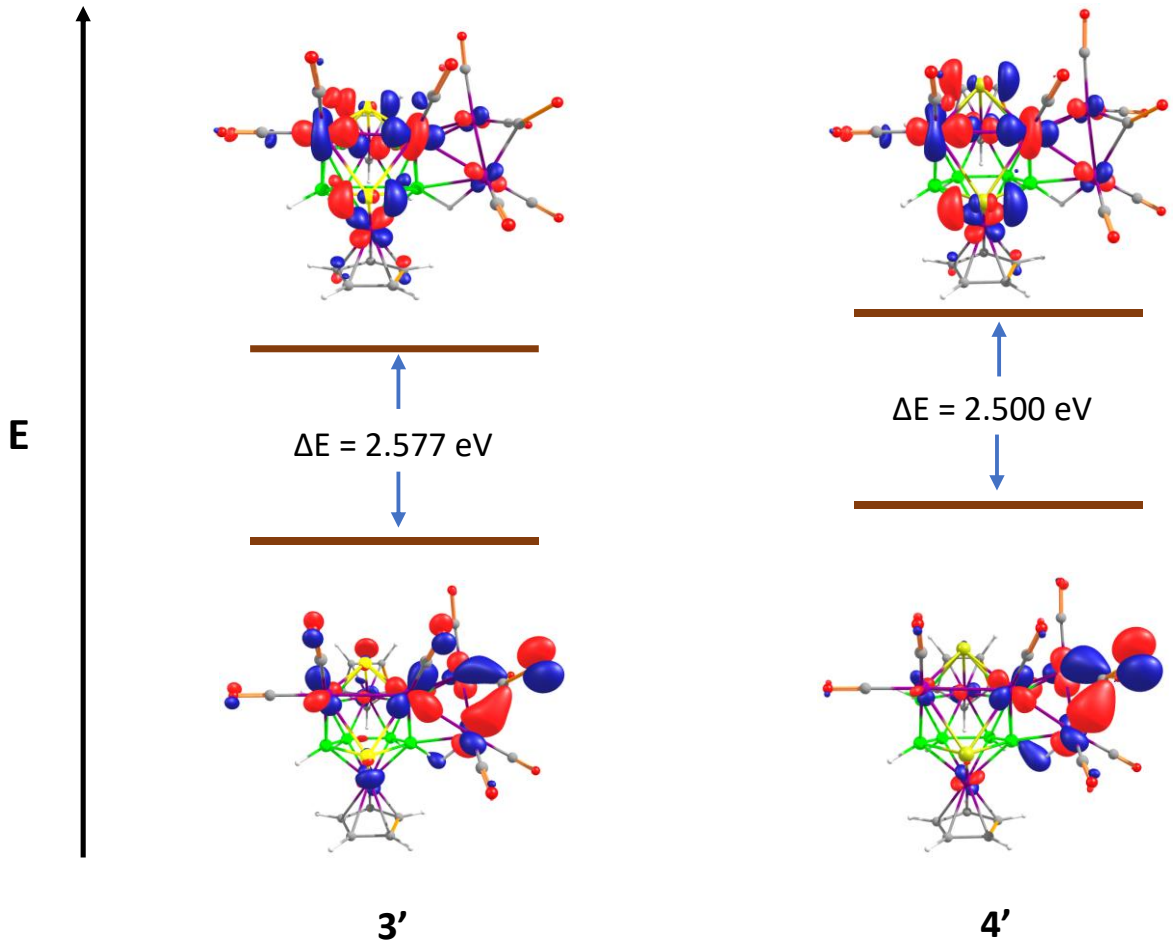

Figure S50. Frontier molecular orbital diagram of **3´** and **4´**. Isosurfaces are plotted at an isovalue of ±0.04 $(e/bohr^3)^{1/2}$.

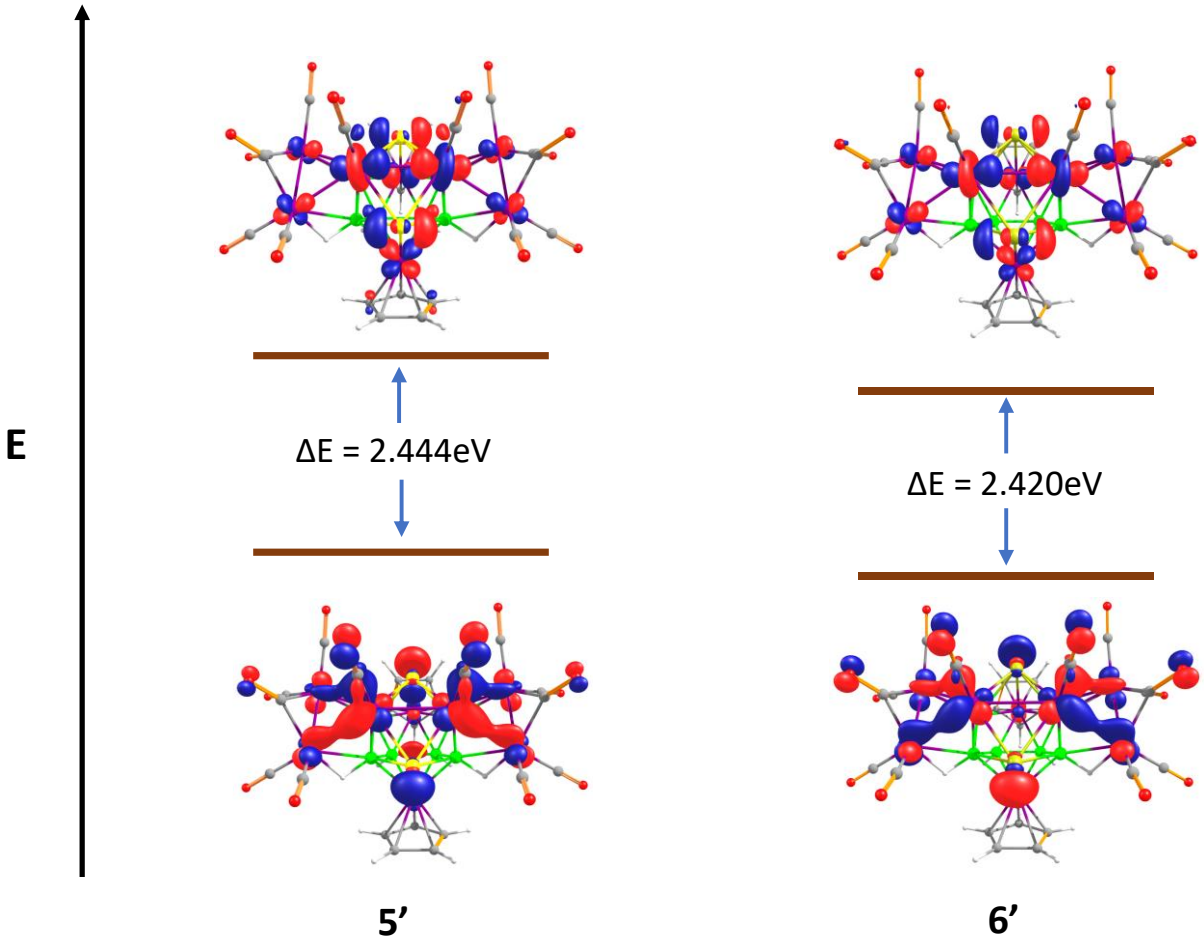

Figure S51. Frontier molecular orbital diagram of **5´** and **6´**. Isosurfaces are plotted at an isovalue of ±0.04 $(e/bohr^3)^{1/2}$.

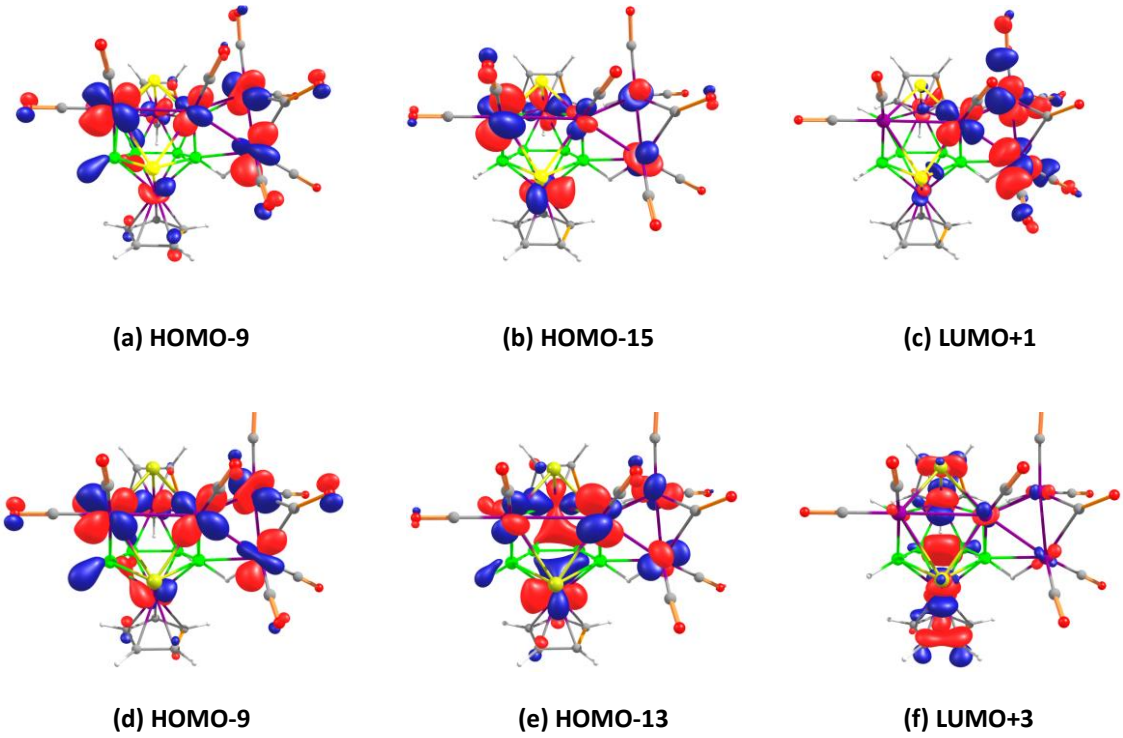

(a) HOMO-9 (b) HOMO-15 (c) LUMO+1

(d) HOMO-9 (e) HOMO-13 (f) LUMO+3

Figure. **S52.** Selected frontier molecular orbitals (a), (b) and (c) for **3´**; and (d), (e) and (f) for **4´**. Isosurfaces are plotted at an isovalue of ±0.04 $(e/bohr^3)^{1/2}$.

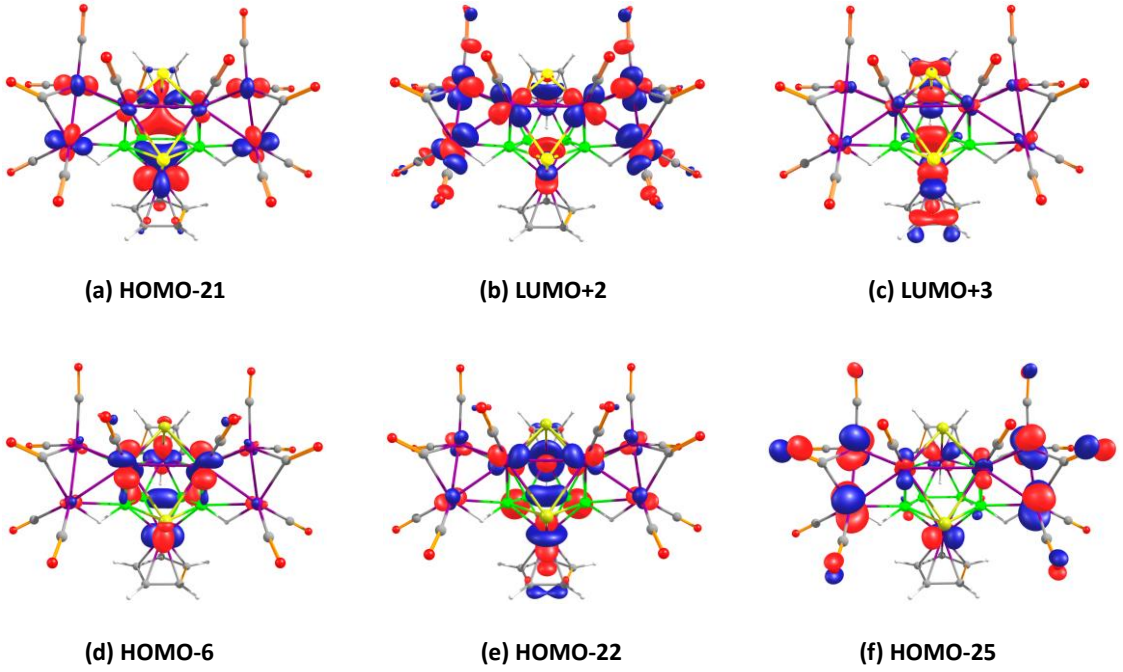

(a) HOMO-21 (b) LUMO+2 (c) LUMO+3

(d) HOMO-6 (e) HOMO-22 (f) HOMO-25

Figure. **S53.** Selected frontier molecular orbitals (a), (b) and (c) for **5´**; and (d), (e) and (f) for **6´**. Isosurfaces are plotted at an isovalue of ±0.04 $(e/bohr^3)^{1/2}$.

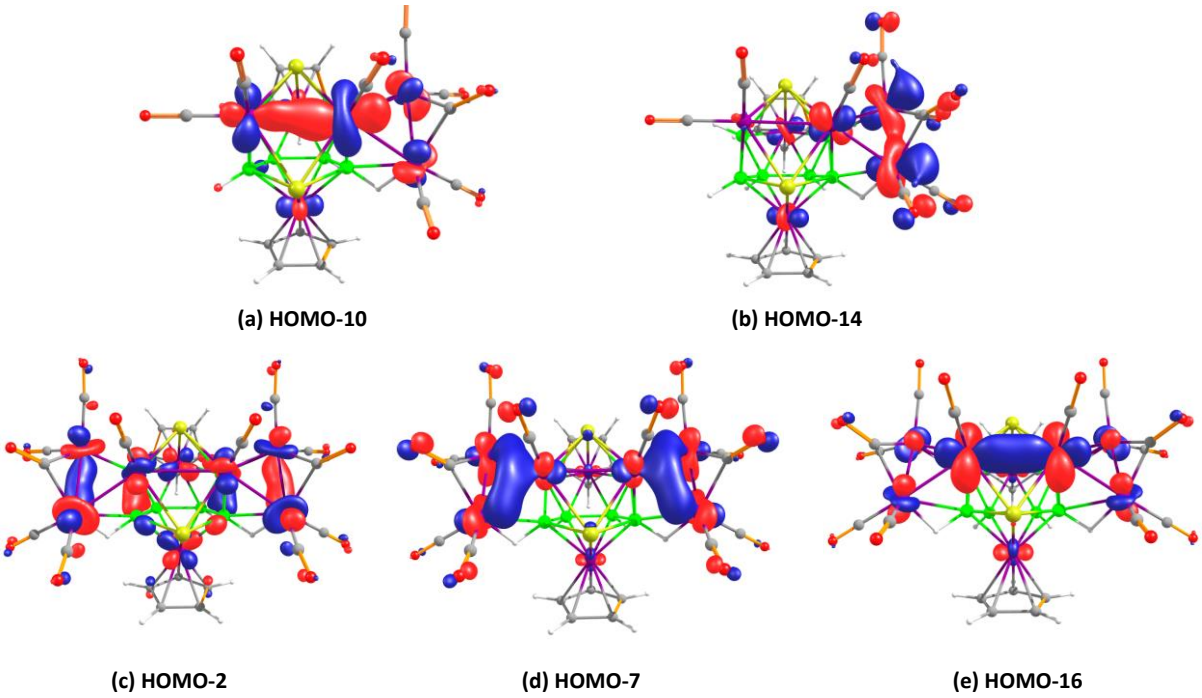

Figure S54. Selected M-M bonding interaction (a) and (b) for **4´**; (c), (d) and (e) for **6´**. Isosurfaces are plotted at an isovalue of ±0.04 $(e/bohr^3)^{1/2}$.

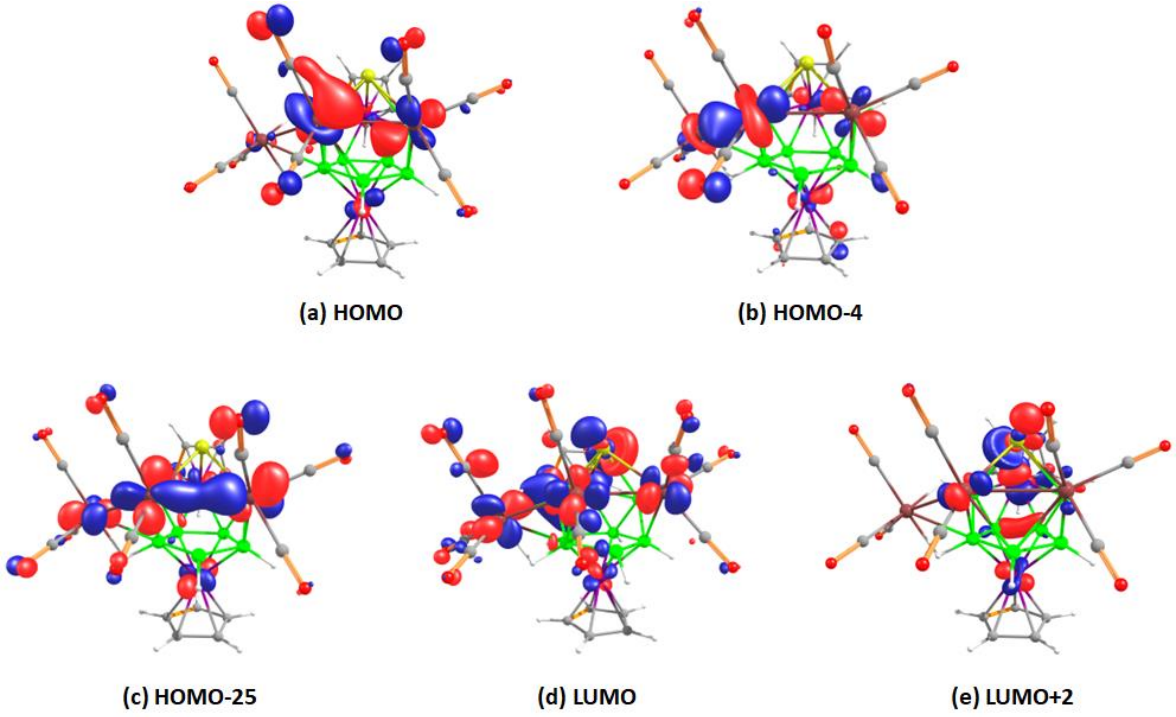

Figure. S55. Selected frontier molecular orbitals (a), (b), (c), (d) and (e) for **8´**. Isosurfaces are plotted at an isovalue of ±0.04 $(e/bohr^3)^{1/2}$.

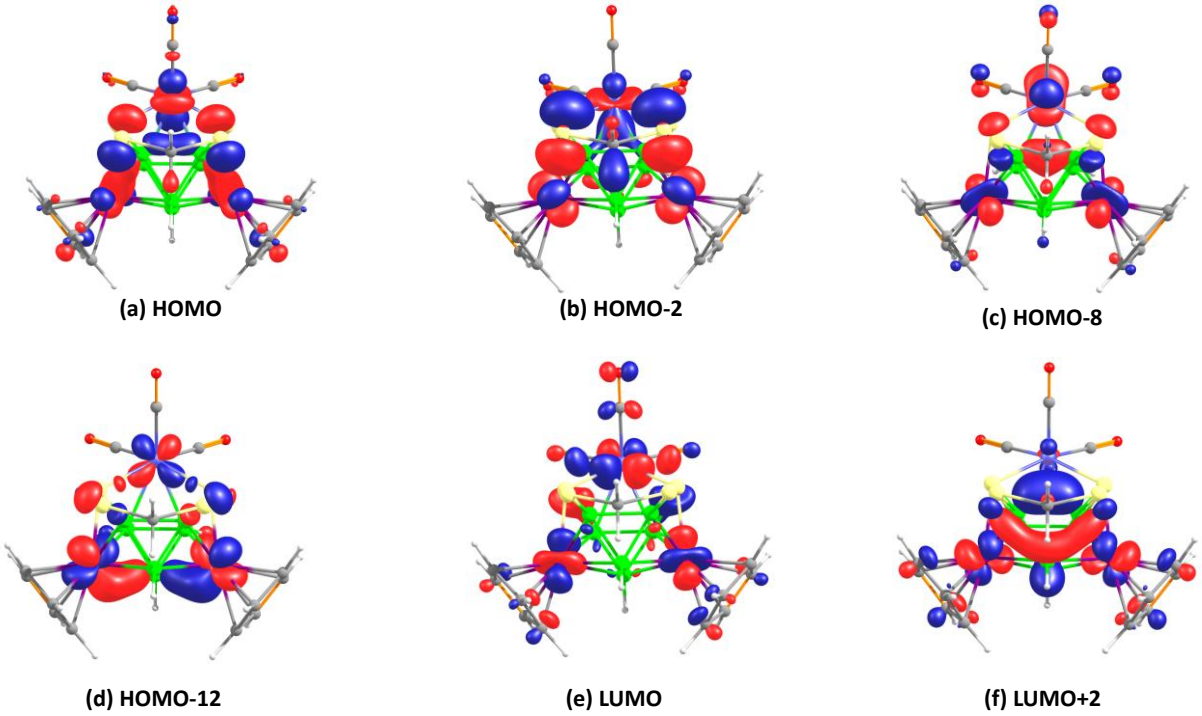

Figure. **S56.** Selected frontier molecular orbitals (a), (b), (c), (d) (e) and (f) for **10´**. Isosurfaces are plotted at an isovalue of ±0.04 $(e/bohr^3)^{1/2}$.

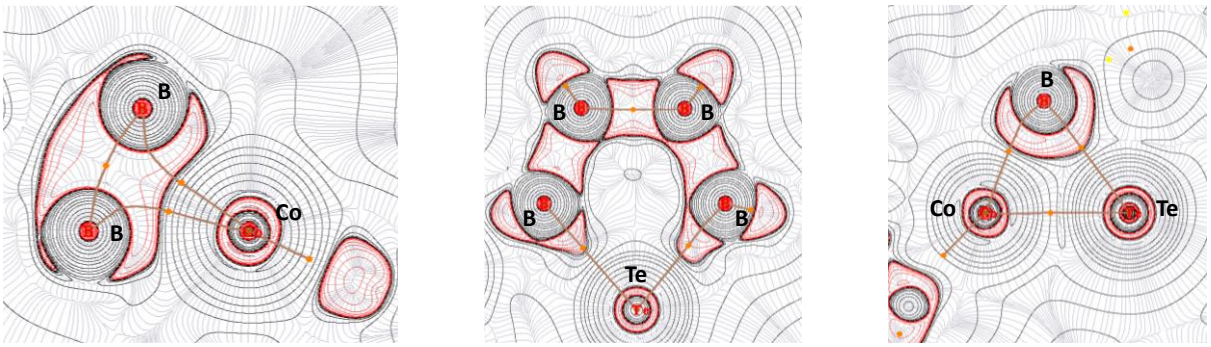

(a) **(b)** **(c)**

Figure. **S57.** Contour-line diagram of the Laplacian of electron density, $\nabla^2\rho(r)$ of (a) Co1-B2-B6 and (b) B3-B4-Te2-B6-B2 planes for **4´** and (c) Co1-Te2-B6 plane for **6´**. The solid brown lines are bond paths, while orange spheres indicate the bond critical points. Area of charge concentration [$\nabla^2\rho(r)<0$] are indicated by solid lines and area of charge depletion [$\nabla^2\rho(r)>0$] are shown by dashed lines.

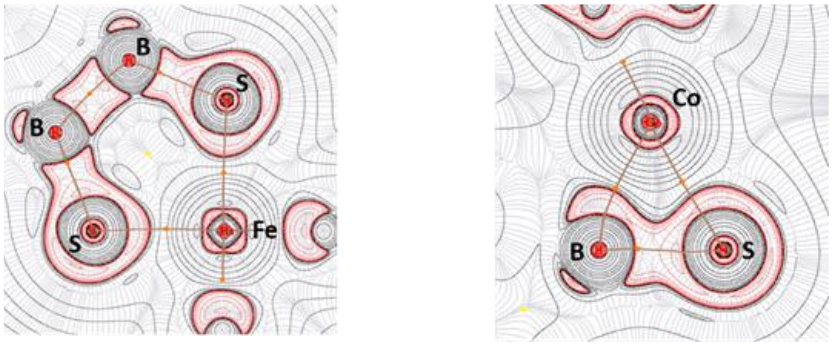

(a) (b)

Figure. **S58.** Contour-line diagram of the Laplacian of electron density, $\nabla^2\rho(r)$ of (a) B3-S1-Fe1-S1-B3 and (b) Co1-B3-S1 planes for **10´**. The solid brown lines are bond paths, while yellow and orange spheres indicate the ring and bond critical points respectively. Area of charge concentration [$\nabla^2\rho(r)<0$] are indicated by solid lines and area of charge depletion [$\nabla^2\rho(r)>0$] are shown by dashed lines.

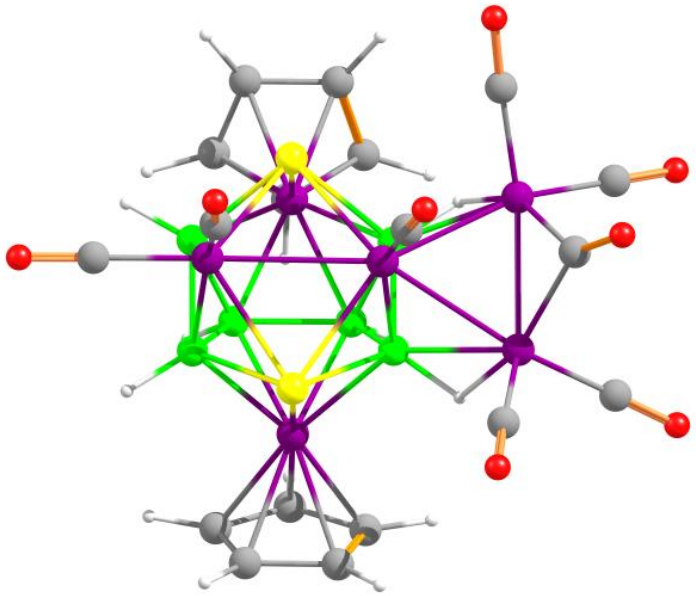

Figure S59. Optimized geometry of **3´**

T. E. = -14547.5149 a. u.

Cartesian coordinates for the calculated structure of **3´** (in Å).

B	0.239486000	-0.862345000	0.832149000
H	-1.101129000	-1.559769000	1.405330000
B	0.902344000	0.000459000	-1.873354000
H	0.690308000	0.003036000	-3.047308000
B	2.543761000	-0.005608000	-1.125667000
H	3.568599000	-0.006872000	-1.735659000
B	2.587034000	0.876384000	0.423713000
H	3.548066000	1.492558000	0.747878000
B	2.583308000	-0.892744000	0.420478000
H	3.541969000	-1.512224000	0.745340000
B	-0.234480000	0.867013000	-0.830369000
H	-1.092316000	1.570397000	-1.401934000
C	1.124702000	3.866342000	-1.811352000
C	1.130167000	3.018737000	-2.942769000
C	2.434920000	2.461069000	-3.062675000
C	3.239904000	2.988060000	-2.015400000
C	2.428231000	3.845263000	-1.237198000
C	1.126739000	-2.997233000	-2.967656000
C	1.084232000	-3.855492000	-1.845187000
C	2.377675000	-3.866240000	-1.248526000
C	3.220399000	-3.018702000	-2.004400000
C	2.444717000	-2.465554000	-3.059952000
C	3.148925000	0.008549000	3.002645000
C	0.775635000	-0.030565000	3.807538000
C	-1.832025000	0.010842000	2.463653000
C	-2.640382000	-2.666159000	0.595385000
C	-3.715960000	0.008909000	0.295463000
C	-3.523756000	-1.709817000	-1.791922000
C	-2.634771000	2.683939000	0.589580000
C	-3.511715000	1.718789000	-1.796989000
Co	1.621409000	1.878320000	-1.239171000
Co	1.610975000	-1.883435000	-1.245520000
Co	1.580333000	-0.006356000	2.217194000
Co	-0.815381000	0.001754000	0.987531000
Co	-2.467997000	-1.211460000	-0.447772000
Co	-2.461595000	1.224207000	-0.447603000
O	4.171202000	0.017289000	3.507577000
O	0.344416000	-0.048754000	4.862556000
O	-2.508136000	0.018324000	3.383119000
O	-2.811689000	-3.570024000	1.268147000
O	-4.735617000	0.011880000	0.858710000
O	-2.807081000	3.590959000	1.257733000
O	-4.186392000	-2.033629000	-2.660826000
O	-4.170307000	2.039440000	-2.670146000
H	2.731300000	4.361664000	-0.340950000
H	4.266255000	2.730527000	-1.815391000
H	0.274509000	4.405872000	-1.426782000
H	0.287129000	2.793986000	-3.574508000
H	2.752057000	1.751987000	-3.808020000
H	0.216641000	-4.381058000	-1.480711000
H	0.299495000	-2.748684000	-3.611211000
H	2.789170000	-1.756025000	-3.792640000
H	4.248294000	-2.784638000	-1.784399000
H	2.654644000	-4.397424000	-0.352454000
Se	0.714486000	1.836785000	0.938473000
Se	0.707471000	-1.841764000	0.932958000

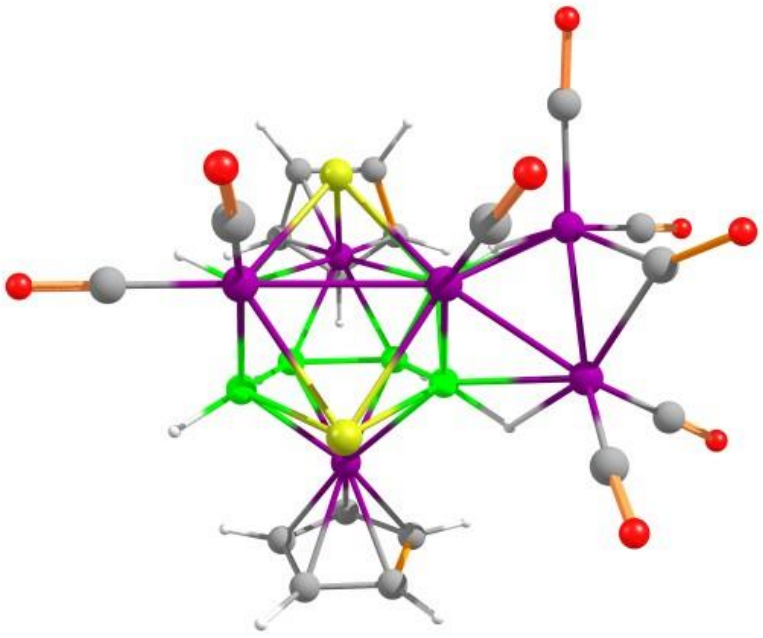

Figure S60. Optimized geometry of **4´**

T. E. = -10277.7761 a. u.

Cartesian coordinates for the calculated structure of **4´** (in Å).

B	0.366666000	0.862061000	-0.903304000
H	1.268788000	1.560197000	-1.446816000
B	-0.711149000	0.000163000	-2.000439000
H	-0.438756000	0.000257000	-3.178564000
B	-2.416254000	-0.000142000	-1.386174000
H	-3.376718000	-0.000356000	-2.119954000
B	-2.633075000	-0.881428000	0.140882000
H	-3.643907000	-1.493008000	0.372346000
B	-2.633471000	0.880926000	0.140925000
H	-3.644513000	1.492006000	0.372780000
B	0.367175000	-0.861284000	-0.903506000
H	1.269430000	-1.558864000	-1.447538000
C	-0.932646000	-3.852993000	-1.998120000
C	-0.848814000	-2.977273000	-3.111076000
C	-2.144817000	-2.412721000	-3.321019000
C	-3.034856000	-2.964083000	-2.350965000
C	-2.285496000	-3.843083000	-1.526898000
C	-0.851454000	2.975764000	-3.112596000
C	-0.932158000	3.852124000	-1.999912000
C	-2.284124000	3.844011000	-1.526177000
C	-3.036103000	2.965521000	-2.348442000
C	-2.148538000	2.412670000	-3.319885000
C	-3.387230000	-0.001729000	2.640758000
C	-1.043473000	0.000651000	3.657156000
C	1.733998000	0.000685000	2.511626000
C	2.725802000	2.681552000	0.604787000
C	3.710113000	0.000499000	0.476089000
C	3.674600000	1.613231000	-1.711987000
C	2.725325000	-2.680243000	0.605425000
C	3.675838000	-1.614034000	-1.711047000
Co	-1.476988000	-1.878055000	-1.420080000
Co	-1.477696000	1.878090000	-1.420014000
Co	-1.749750000	-0.000420000	2.017663000
Co	0.839492000	0.000011000	0.956514000
Co	2.545927000	1.207466000	-0.401169000
Co	2.546344000	-1.206712000	-0.401352000
O	-4.461503000	-0.002664000	3.038293000
O	-0.650451000	0.001329000	4.733220000
O	2.315232000	0.001139000	3.500258000
O	2.915312000	3.602592000	1.260206000
O	4.668896000	0.000609000	1.147794000
O	2.914206000	-3.600934000	1.261526000
O	4.389618000	1.881533000	-2.565873000
O	4.391377000	-1.883512000	-2.564120000
H	-2.667471000	-4.396257000	-0.670172000
H	-4.085643000	-2.709868000	-2.229412000
H	-0.108892000	-4.417533000	-1.563775000
H	0.049598000	-2.740273000	-3.677491000
H	-2.405226000	-1.681992000	-4.083017000
H	-0.106912000	4.415828000	-1.567318000
H	0.045611000	2.737377000	-3.680557000
H	-2.411228000	1.681912000	-4.081073000
H	-4.086968000	2.712621000	-2.224815000
H	-2.663824000	4.398098000	-0.669027000
Te	-0.688704000	2.023843000	0.973740000
Te	-0.687988000	-2.024150000	0.973637000

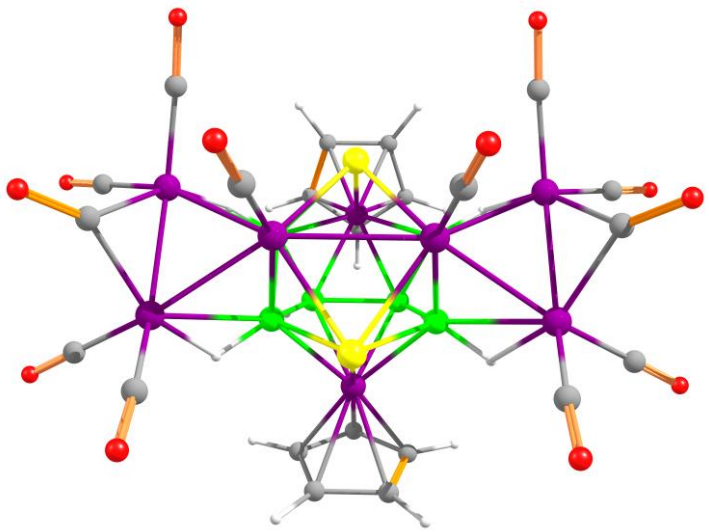

Figure S61. Optimized geometry of **5´**

T. E. = -17766.7714 a. u.

Cartesian coordinates for the calculated structure of **5´** (in Å).

Co	-1.885415000	1.927692000	0.000000000
Co	-1.217185000	-0.441496000	3.429901000
Co	0.000033000	-1.084163000	1.347491000
Se	-1.828276000	-0.433221000	0.000000000
C	-3.865329000	2.238117000	-0.712144000
C	-3.021307000	3.284174000	-1.152004000
C	-2.484201000	3.923170000	0.000000000
C	0.000079000	-2.867230000	1.567337000

C	-2.693283000	-1.440209000	3.176678000	C	2.693359000	-1.440097000	-3.176671000
C	0.000044000	-1.663662000	4.218083000	C	0.000044000	-1.663662000	-4.218083000
C	-1.686256000	0.341352000	4.959043000	C	1.686259000	0.341410000	-4.959044000
O	-1.989414000	0.851829000	5.931499000	O	1.989381000	0.851878000	-5.931516000
O	0.000063000	-2.622992000	4.878410000	O	0.000063000	-2.622992000	-4.878410000
O	-3.607911000	-2.111543000	3.073408000	O	3.608021000	-2.111383000	-3.073378000
O	-0.000219000	-3.997347000	1.714749000	O	-0.000219000	-3.997347000	-1.714749000
B	-0.863423000	0.820307000	1.549549000	C	3.865255000	2.238276000	-0.712144000
B	-0.000037000	2.231857000	0.902487000	C	3.021188000	3.284297000	-1.152004000
H	-0.000057000	3.222042000	1.567284000	Co	1.217220000	-0.441449000	3.429897000
H	-1.549930000	1.008001000	2.573115000	C	2.693359000	-1.440097000	3.176671000
Se	1.828314000	-0.433149000	0.000000000	C	1.686259000	0.341410000	4.959044000
B	0.863404000	0.820339000	-1.549547000	O	1.989381000	0.851878000	5.931516000
B	-0.000037000	2.231857000	-0.902487000	O	3.608021000	-2.111383000	3.073378000
H	-0.000057000	3.222042000	-1.567284000	Co	-1.217185000	-0.441496000	-3.429901000
H	1.549903000	1.008062000	-2.573115000	C	-2.693283000	-1.440209000	-3.176678000
B	0.863404000	0.820339000	1.549547000	C	-1.686256000	0.341352000	-4.959043000
H	1.549903000	1.008062000	2.573115000	O	-1.989414000	0.851829000	-5.931499000
B	-0.863423000	0.820307000	-1.549549000	O	-3.607911000	-2.111543000	-3.073408000
H	-1.549930000	1.008001000	-2.573115000	H	1.782020000	4.739379000	0.000000000
C	-3.865329000	2.238117000	0.712144000	H	2.785537000	3.525126000	-2.175065000
C	-3.021307000	3.284174000	1.152004000	H	4.391735000	1.540082000	-1.342412000
Co	1.885352000	1.927768000	0.000000000	H	4.391735000	1.540082000	1.342412000
Co	1.217220000	-0.441449000	-3.429897000	H	2.785537000	3.525126000	2.175065000
Co	0.000033000	-1.084163000	-1.347491000	H	-2.785667000	3.525012000	-2.175065000
C	3.865255000	2.238276000	0.712144000	H	-1.782197000	4.739306000	0.000000000
C	3.021188000	3.284297000	1.152004000	H	-2.785667000	3.525012000	2.175065000
C	2.484057000	3.923272000	0.000000000	H	-4.391778000	1.539902000	1.342415000
C	0.000079000	-2.867230000	-1.567337000	H	-4.391778000	1.539902000	-1.342415000

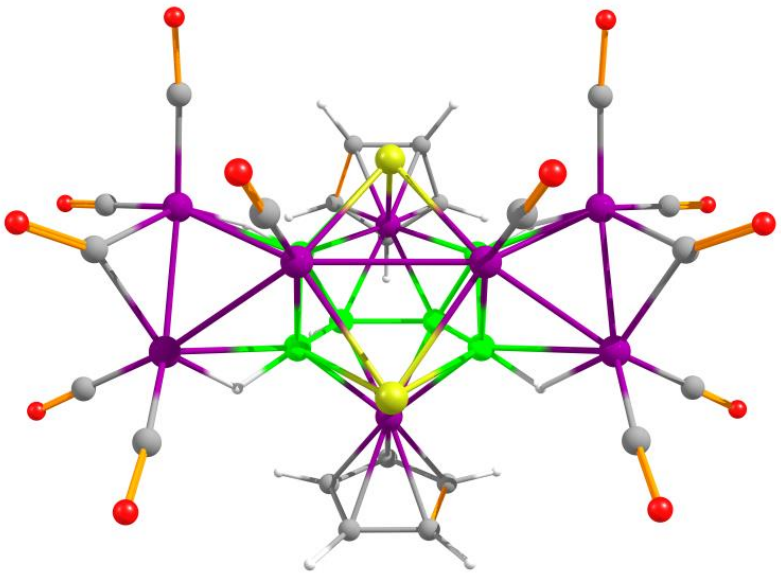

Figure S62. Optimized geometry of **6´**

T. E. = -13499.8216 a. u.

Cartesian coordinates for the calculated structure of **6´** (in Å).

Te	1.986572000	0.000000000	-0.583952000	Co	1.220324000	-3.496050000	-0.355809000
Co	1.890860000	0.000000000	1.932508000	O	0.000000000	1.781821000	-3.986482000
Co	0.000000000	1.424987000	-1.068903000	O	3.639483000	-3.319281000	-2.009885000

O	1.917604000	-5.972581000	1.022151000
O	0.000000000	-4.932390000	-2.545572000
C	2.452667000	0.000000000	3.947678000
C	3.000184000	-1.151923000	3.319208000
C	3.862262000	-0.713197000	2.288420000
C	0.000000000	1.648558000	-2.854324000
C	2.713537000	-3.341141000	-1.345005000
C	1.641533000	-5.010176000	0.478221000
C	0.000000000	-4.274615000	-1.584099000
B	0.856390000	-1.588532000	0.863429000
H	1.526782000	-2.620690000	1.084243000
B	0.000000000	-0.907156000	2.245771000
H	0.000000000	-1.533200000	3.261794000
Te	-1.986572000	0.000000000	-0.583952000
B	-0.856390000	1.588532000	0.863429000
H	-1.526782000	2.620690000	1.084243000
B	0.000000000	0.907156000	2.245771000
H	0.000000000	1.533200000	3.261794000
B	0.856390000	1.588532000	0.863429000
H	1.526782000	2.620690000	1.084243000
B	-0.856390000	-1.588532000	0.863429000
H	-1.526782000	-2.620690000	1.084243000
C	3.000184000	1.151923000	3.319208000
C	3.862262000	0.713197000	2.288420000
Co	-1.890860000	0.000000000	1.932508000
Co	0.000000000	-1.424987000	-1.068903000
Co	-1.220324000	3.496050000	-0.355809000
O	0.000000000	-1.781821000	-3.986482000
O	-3.639483000	3.319281000	-2.009885000
O	-1.917604000	5.972581000	1.022151000
O	0.000000000	4.932390000	-2.545572000
C	-2.452667000	0.000000000	3.947678000
C	-3.000184000	1.151923000	3.319208000
C	-3.862262000	0.713197000	2.288420000
C	0.000000000	-1.648558000	-2.854324000
C	-2.713537000	3.341141000	-1.345005000
C	-1.641533000	5.010176000	0.478221000
C	0.000000000	4.274615000	-1.584099000
C	-3.000184000	-1.151923000	3.319208000
C	-3.862262000	-0.713197000	2.288420000
Co	1.220324000	3.496050000	-0.355809000
O	3.639483000	3.319281000	-2.009885000
O	1.917604000	5.972581000	1.022151000
C	2.713537000	3.341141000	-1.345005000
C	1.641533000	5.010176000	0.478221000
Co	-1.220324000	-3.496050000	-0.355809000
O	-3.639483000	-3.319281000	-2.009885000
O	-1.917604000	-5.972581000	1.022151000
C	-2.713537000	-3.341141000	-1.345005000
C	-1.641533000	-5.010176000	0.478221000
H	-1.735739000	0.000000000	4.750585000
H	-2.761382000	2.174823000	3.557253000
H	-4.411297000	1.344582000	1.608893000
H	-4.411297000	-1.344582000	1.608893000
H	-2.761382000	-2.174823000	3.557253000
H	1.735739000	0.000000000	4.750585000
H	2.761382000	-2.174823000	3.557253000
H	4.411297000	-1.344582000	1.608893000
H	4.411297000	1.344582000	1.608893000
H	2.761382000	2.174823000	3.557253000

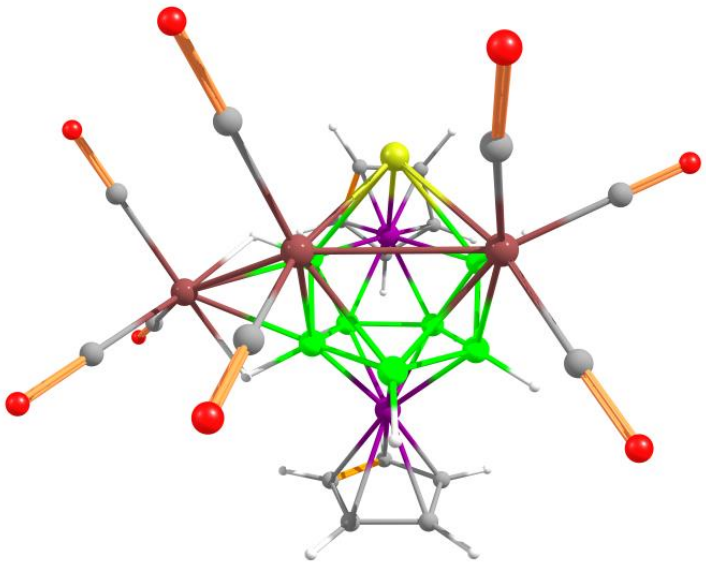

Figure S63. Optimized geometry of **8´**

T. E. = -4791.5563 a. u.

Cartesian coordinates for the calculated structure of **8´** (in Å).

Co	-0.465942000	2.065625000	-1.600974000
Co	-0.060426000	1.774461000	2.105690000
Ru	-2.396219000	-1.023084000	0.368728000
Ru	2.898578000	-0.383605000	-0.147348000

Ru	0.412803000	-1.569215000	0.049102000
Te	-1.043969000	-0.359223000	-1.883545000
C	-0.776292000	3.160502000	3.537746000
C	-0.536892000	1.915575000	4.173737000
C	0.837041000	1.602754000	4.023837000
C	1.453656000	2.662308000	3.302845000
C	0.456620000	3.623269000	3.004123000
C	-0.096964000	4.071188000	-2.016736000
C	0.800656000	3.277305000	-2.783357000
C	0.030548000	2.455384000	-3.638042000
C	-1.346543000	2.754789000	-3.414649000
C	-1.425213000	3.756793000	-2.422690000
C	3.667119000	-1.622193000	1.067663000
C	4.356348000	0.902579000	-0.142520000
C	3.469444000	-1.439214000	-1.636214000
C	0.709021000	-2.685851000	1.534558000
C	0.688306000	-3.047088000	-1.132165000
C	-2.987620000	-1.382367000	2.140472000
C	-2.347105000	-2.900114000	-0.098045000
C	-4.183781000	-0.709015000	-0.254749000
O	-3.368868000	-1.593738000	3.192894000
O	-5.251558000	-0.538684000	-0.616830000
O	-2.431809000	-4.006328000	-0.368430000
O	0.869224000	-3.941031000	-1.827803000
O	0.864378000	-3.370046000	2.440313000
O	3.818168000	-2.061026000	-2.524460000
O	4.142505000	-2.353847000	1.799598000
O	5.231140000	1.631453000	-0.137672000
B	-0.533264000	-0.208522000	1.717056000
H	-0.527066000	-0.748595000	2.775680000
B	0.924906000	0.446859000	0.905910000
H	2.162575000	0.375453000	1.338936000
B	0.873234000	0.636035000	-0.796810000
H	1.963431000	0.595029000	-1.449394000
B	-1.862534000	1.069573000	1.328263000
H	-2.750651000	1.361138000	2.069627000
B	0.619322000	2.058680000	0.199313000
H	1.524423000	2.834969000	0.141502000
B	-1.105280000	2.427519000	0.426153000
H	-1.542357000	3.532408000	0.532782000
B	-2.187434000	1.310142000	-0.368527000
H	-3.192714000	1.657993000	-0.890282000
H	0.413924000	1.722959000	-4.329930000
H	1.874140000	3.274861000	-2.693869000
H	0.178820000	4.779752000	-1.254837000
H	-2.327881000	4.172546000	-2.008463000
H	-2.183312000	2.281003000	-3.901775000
H	-1.730729000	3.650537000	3.443533000
H	-1.279960000	1.289923000	4.639228000
H	1.320760000	0.704190000	4.369706000
H	2.488833000	2.712266000	3.007824000
H	0.598593000	4.525521000	2.432927000

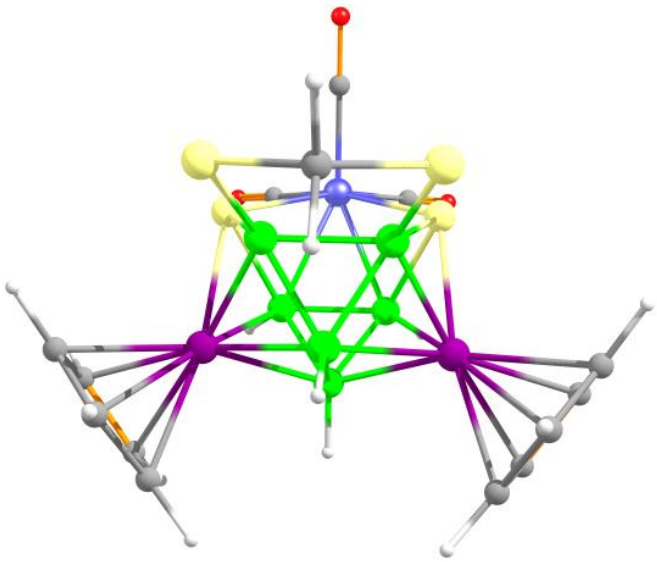

Figure S64. Optimized geometry of **10´**

T. E. = -6540.8196 a. u.

Cartesian coordinates for the calculated structure of **10´** (in Å).

Co	0.930683000	-1.878374000	-0.672629000
Fe	-2.481805000	0.000189000	0.040167000
S	-0.920984000	-1.683329000	0.579518000
S	1.399231000	-1.524815000	2.789534000
O	-3.667652000	0.000266000	2.762336000
O	-4.209788000	2.052565000	-1.159882000
C	0.804012000	-3.857932000	-1.485244000
C	1.552762000	-3.875888000	-0.268631000
C	2.673102000	-3.034838000	-0.434134000
C	2.605974000	-2.475916000	-1.744436000
C	1.463361000	-3.015672000	-2.402403000
C	-3.192141000	0.000220000	1.730108000

C	-3.534805000	1.256442000	-0.704578000
C	2.294755000	-0.000189000	3.255720000
H	2.406581000	-0.000204000	4.338295000
H	3.281039000	-0.000259000	2.796376000
B	-0.889018000	-0.876843000	-1.298921000
H	-1.371977000	-1.528801000	-2.163642000
B	0.645753000	-0.000038000	-1.565857000
H	1.051578000	-0.000060000	-2.685697000
B	0.712284000	-0.926665000	1.178953000
B	1.603844000	-0.000117000	-0.042439000
H	2.785224000	-0.000206000	0.129812000
S	-0.920729000	1.683471000	0.579541000
S	1.399462000	1.524576000	2.789555000
B	-0.888887000	0.876998000	-1.298912000
H	-1.371749000	1.529045000	-2.163620000
B	0.712430000	0.926556000	1.178961000
Co	0.930961000	1.878250000	-0.672609000
O	-4.210155000	-2.051921000	-1.159800000
C	0.804624000	3.857762000	-1.485396000
C	1.553235000	3.875725000	-0.268696000
C	2.673496000	3.034530000	-0.434000000
C	2.606446000	2.475499000	-1.744258000
C	1.463982000	3.015353000	-2.402409000
C	-3.534978000	-1.255919000	-0.704573000
H	-0.130237000	4.367379000	-1.654744000
H	1.289089000	4.409336000	0.629664000
H	3.406021000	2.801074000	0.320057000
H	1.126454000	2.763884000	-3.393715000
H	3.302925000	1.769920000	-2.164911000
H	1.125747000	-2.764242000	-3.393690000
H	-0.130933000	-4.367447000	-1.654441000
H	1.288654000	-4.409391000	0.629804000
H	3.405742000	-2.801408000	0.319818000
H	3.302495000	-1.770461000	-2.165229000

References

(1) Zafar, M.; Kar, S.; Nandi, C.; Ramalakshmi, R.; Ghosh, S. Cluster Fusion: Face-fused Macropolyhedral Tetracobaltaboranes. *Inorg. Chem*. **2019**, *58*, 47-51.

(2) Kaur, P.; Thornton-Pett, M.; Clegg, W.; Kennedy, J. D. Macropolyhedral boron-containing cluster chemistry: nineteen-vertex $[(PPh_3)NiS_2B_{16}H_{12}(PPh_3)]$ and eighteen-vertex $S_2B_{16}H_{14}(PPh_3)$, *J. Chem. Soc. Dalton Trans.* **1996**, *1996*, 4155–4157.

(3) Barton, L.; Bould, J.; Kennedy, J. D.; Rath, N. P. Macropolyhedral boron-containing cluster chemistry. Isolation and characterisation of the eighteen-vertex nido-5′-iridaoctaborano [3′,8′:1′,2]-closo-4-iridadodec aborane, $[(CO)(PMe_3)_2IrB_{16}H_{14}Ir(CO)(PMe_3)_2]$. *J. Chem. Soc. Dalton Trans.* **1996**, 3145−3149.

(4) Nandi, C.; Kar, S.; Zafar, M.; Kar, K.; Roisnel, T.; Dorcet, V.; Ghosh, S. Chemistry of Dimetallaoctaborane(12) with Chalcogen-Based Borate Ligands: Obedient versus Disobedient Clusters. *Inorg. Chem.* **2020**, *59*, 3537-3541.

(5) di Biani, F. F.; Laschi, F.; Zanello, P.; Ferguson, G.; Trotter, J.; O'Riordand, G. M.; Spalding, T. R. Synthesis, structure, spectroscopic and electrochemical study of the paramagnetic compound $[2\text{-}(\eta^7\text{-}C_7H_7)\text{-}7,11\text{-}F_2\text{-}2,1\text{-}closo\text{-}MoTeB_{10}H_8]$. *J. Chem. Soc. Dalton Trans.* **2001**, 1520-1523.

(6) Joseph, B.; Barik, S. K.; Ramalakshmi, R.; Kundu, G.; Roisnel, T.; Dorcet, V.; Ghosh, S. Chemistry of Triple-Decker Sandwich Complexes Containing Four-Membered Open B_2E_2 Rings (E = S or Se). *Eur. J. Inorg. Chem*. **2018**, 2045–2053.

(7) (a) Led, J. J.; Gesmar, H. Application of the Linear Prediction Method to NMR Spectroscopy. *Chem. Rev.* **1991**, *91*, 1413-1426. (b) Yang, L.; Simionescua, R.; Lough, A.; Yan, H. Some observations relating to the stability of the BODIPY uorophore under acidic and basic conditions. *Dyes and Pigments* **2011**, *91*, 264-267. (c) Weiss, R.; Grimes, R. N. Sources of Line Width in Boron-11 Nuclear Magnetic Resonance Spectra. Scalar Relaxation and Boron-Boron Coupling in B_4H_{10} and B_5H_9. *J. Am. Chem. Soc.* **1978**, *100*, 1401-1405.

(8) Frisch, M. J.; Trucks, G. W.; Schlegel, H. B.; Scuseria, G. E.; Robb, M. A.; Cheeseman, J. R.; Scalmani, G.; Barone, V.; Mennucci, B.; Petersson, G. A.; Nakatsuji, H.; Caricato, M.; Li, X.; Hratchian, H. P.; Izmaylov, A. F.; Bloino, J.; Zheng, G.; Sonnenberg, J. L.; Hada, M.; Ehara, M.; Toyota, K.; Fukuda, R.; Hasegawa, J.; Ishida, M.; Nakajima, T.; Honda, Y.; Kitao, O.; Nakai, H.; Vreven, T.; Montgomery, J. A.; Peralta, Jr., J. E.; Ogliaro, F.; Bearpark, M.; Heyd, J. J.; Brothers, E.; Kudin, K. N.; Staroverov, V. N.; Keith, T.; Kobayashi, R.; Normand, J.; Raghavachari, K.; Rendell, A.; Burant, J. C.; Iyengar, S. S.; Tomasi, J.; Cossi, M.; Rega, N.; Millam, J. M.; Klene, M.; Knox, J. E.; Cross, J. B.; Bakken, V.; Adamo, C.; Jaramillo, J.; Gomperts, R.; Stratmann, R. E.; Yazyev, O.; Austin, A. J.; Cammi, R.; Pomelli, C.; Ochterski, J. W.; Martin, R. L.; Morokuma, K.; Zakrzewski, V. G.; Voth, G. A.; Salvador, P.; Dannenberg, J. J.; Dapprich, S.; Daniels, A. D.; Farkas, O.; Foresman, J. B.; Ortiz, J. V.; Cioslowski, J. ; Fox, D. J. Gaussian16, Rev. B.01; Gaussian, Inc., Wallingford CT, 2016.

(9) Lee, C.; Yang, W.; Parr. R. G. Development of the Colle-Salvetti correlation-energy formula into a functional of the electron density. *Phys. Rev. B.* **1988**, *37*, 785-789.

(10) EMSL Basis Set Exchange Library. https://bse.pnl.gov/bse/portal.

(11) (a) London, F. J., Théorie quantique des courants interatomiques dans les combinaisons aromatiques. J. Phys. Radium 1937, 8, 397-409. b) Ditchfield, R. Self-consistent perturbation theory of diamagnetism. Mol. Phys. 1974, 27, 789-807. c) Wolinski, K.; Hinton J. F.; Pulay, P. Efficient Implementation of the Gauge-Independent Atomic Orbital Method for NMR Chemical Shift Calculations. *J. Am. Chem. Soc.* **1990**, *112*, 8251-8260.

(12) Onak, T. P.; Landesman, H. L.; Williams, R. E.; Shapiro, I. The B11 Nuclear Magnetic Resonance Chemical Shifts and Spin Coupling Values for Various Compounds. *J. Phys. Chem.* **1959**, *63*, 1533-1535.

(13) Wiberg, K., Application of the pople-santry-segal CNDO method to the cyclopropylcarbinyl and cyclobutylcation and to bicyclobutane. *Tetrahedron* **1968**, *24*, 1083-1096.

(14) (a) Weinhold, F.; Landis, C. R. Valency and bonding: A natural bond orbital donor-acceptor perspective; Cambridge University Press: Cambridge, U.K., 2005. (b) Reed, A. E.; Curtiss, L. A.; Weinhold, F. intermolecular Interactions from a Natural Bond Orbital, Donor-Acceptor Viewpoint. *Chem. Rev.* **1988**, *88*, 899-926.

(15) Chemcraft - Graphical Software for Visualization of Quantum Chemistry Computations. https://www.chemcraftprog.com.

(16) Lu, T.; Chen, F. Multiwfn: A multifunctional wavefunction analyzer. J. Comput. Chem. **2012**, *33*, 580-592.